Interplays between nitric oxide and reactive oxygen species in cryptogein signaling

Anna Kulik[1], Elodie Noirot[1], Vincent Grandperret[2], Stéphane Bourque[2], Jérôme Fromentin[1], Pauline Salloignon[3], Caroline Truntzer[3], Grażyna Dobrowolska[4], Françoise Simon-Plas[1] and David Wendehenne[2,§]

[1]INRA, UMR 1347 Agroécologie, Pôle Mécanisme et Gestion des Interactions Plantes-microorganismes - ERL CNRS 6300, 17 rue Sully, BP 86510, 21065 Dijon cédex, France

[2]Université de Bourgogne, UMR 1347 Agroécologie, Pôle Mécanisme et Gestion des Interactions Plantes-microorganismes - ERL CNRS 6300, 17 rue Sully, BP 86510, 21065 Dijon cédex, France

[3]CLIPP (Clinical and Innovation Proteomic Platform), IFR 100 Santé-STIC, 1, rue du Professeur Marion 21000 Dijon, France

[4]Institute of Biochemistry and Biophysics, Polish Academy of Sciences, Pawińskiego 5a, 02-106 Warsaw, Poland

[§]Corresponding author: wendehen@dijon.inra.fr

Running Head: NO and ROS cross-talk in cryptogein signaling

ABSTRACT

The cellular messenger nitric oxide (NO) has many functions in plants. In this study, we investigated its interplays with Reactive Oxygen Species (ROS) in the defense responses triggered by the elicitin cryptogein produced by the oomycete *Phytophthora cryptogea*. The production of NO induced by cryptogein in tobacco cell suspensions was partly regulated through a ROS-dependent pathway involving the NADPH oxidase NtRBOHD. In turn, NO down-regulated the level of H_2O_2 derived from NtRBOHD activity. Both NO and ROS synthesis appeared to be under the control of two redundant isoforms of histone deacetylases of type 2 acting as negative regulators of cell death. Occurrence of an interplay between NO and ROS was further supported by the finding that cryptogein triggered a fast production of peroxynitrite ($ONOO^-$) resulting from the coupling reaction of superoxide ($O_2^{\bullet-}$) with NO. We provided evidence that ROS, but not NO, negatively regulate the intensity of activity of the protein kinase NtOSAK, a member of the SnRK2 protein kinase family. Furthermore, using a micro-array approach, we next identified fifteen genes early induced by cryptogein *via* NO. Interestingly, only a part of these genes was also modulated by ROS derived from NtRBOHD activity and encoded proteins showing sequence identity to ubiquitin ligases. Expression of those genes appeared to be negatively regulated by $ONOO^-$, suggesting that $ONOO^-$ mitigate the effects of NO and ROS in cell response to cryptogein. Finally, we provided evidence that NO required NtRBOHD activity for inducing cell death, thus confirming previous assumption that ROS channel NO through cell death pathways.

Keywords: cell death, cryptogein, defense responses, histone deacetylase, NADPH oxidase, nitric oxide, peroxynitrite, reactive oxygen species, signaling

44 **INTRODUCTION**

45

46 Nitric oxide (NO) is an endogenously produced ubiquitous free radical gas which plays key
47 roles in various physiological processes in plants such as germination, root development, stomatal
48 closure, flowering, hormone signaling or iron homeostasis (Besson-Bard et al. 2008a). Also, it has
49 emerged as a molecule of interest in plant pathology (Bellin et al. 2013). Indeed, NO is rapidly
50 produced in plant cells facing pathogen attack or elicited by MAMPs (Microbe-Associated Molecular
51 Patterns) or DAMPs (Danger-Associated Molecular Patterns; Jeandroz et al. 2013). Its production
52 involves nitrate reductase (Yamamoto-Katou et al. 2006; Perchepied et al. 2010; Rasul et al. 2012)
53 and, according to several studies, a still unidentified enzyme displaying functional similarities with
54 nitric oxide synthase (NOS), the main enzymatic source for NO in animals (Asai & Yoshioka, 2009;
55 Corpas et al. 2009). Mounting evidences indicate that NO serves as a key messenger in plant defense.
56 Supporting this statement, interplays between NO and major components of plant immune signaling
57 pathways such as the second messengers Ca^{2+}, cyclic AMP and cyclic GMP, MAP (Mitogen Activated
58 Protein) kinases, signaling lipids and the hormones salicylic acid, jasmonic acid or ethylene have been
59 widely reported (Mur et al. 2008; Gaupels et al. 2011a; Yoshioka et al. 2011; Mandal et al. 2012; Yun
60 et al. 2012). Through its signaling activity, NO seems to play a part in various stages of plant defense.
61 It indeed contributes to early defense responses as well as to ultimate events including the
62 hypersensitive response (HR) and systemic acquired resistance (SAR; Song & Goodman, 2001;
63 Delledonne et al. 2003; Piterková et al. 2009). Although a role for NO in controlling disease resistance
64 has been established in several pathosystems (Delledonne et al. 1998; Asai et al. 2009; Perchepied et
65 al. 2010; Rasul et al. 2012), subtle processes underlying its functions remain poorly understood.
66 Identification and functional analysis of NO-responsive genes provided significant progresses in
67 understanding its role at a molecular level (Zago et al. 2006; Palmieri et al. 2008; Besson-Bard et al.
68 2009). Notably, these studies confirm the first hints (Delledonne et al. 1998; Durner et al. 1998) that
69 NO regulates the expression of defense genes such as those encoding proteins related to secondary
70 metabolism or pathogenesis-related proteins. Recently, these analysis were completed by the
71 characterization of proteins regulated through NO-dependent processes at the post-translational
72 level by S-nitrosylation and tyrosine nitration (Romero-Puertas et al. 2007; Lindermay & Durner,
73 2009; Vandelle & Delledonne, 2011; Astier et al. 2012a; Skelly & Loake, 2013). Of importance, several
74 of them have important known implications in plant defense such as NPR1 (Nonexpresser of
75 Pathogenesis-Related gene 1) and the NADPH oxidase AtRBOHD (Tada et al. 2008; Lindermayr et al.
76 2010; Yun et al. 2011), thus providing a new view of how NO impacts plant defense responses.

77 Several lines of research highlighted the existence of cross-talks operating between NO and
78 reactive oxygen species (ROS) including superoxide ($O_2^{\bullet-}$) and hydrogen peroxide (H_2O_2) which

79 production result mainly from the activity of NADPH oxidases and superoxide dismutases (SOD),
80 respectively (Mittler et al. 2011). Basically, these species share several similarities,
81 complementarities, but also show contrasting or independent effects. First, their productions occur
82 simultaneously and constitute one of the earliest plant immune responses (Foissner et al. 2000;
83 Delledonne et al. 2001). Second, both species display signaling functions and, for instance, were
84 shown to regulate unique as well as common set of genes (Zago et al. 2006). Third, unregulated
85 synthesis of these species has been implicated as causal or contributing to improper defense
86 responses (see for instance Takahashi et al. 1997; Chamnongpol et al. 1998; Asai & Yoshioka, 2009;
87 Rasul et al. 2012). Fourth, ROS and NO, as well as other reactive nitrogen species (RNS), have distinct
88 reactivities and also abilities to freely cross membranes, depending on their chemical nature
89 (Hughes, 2008; Ferrer-Sueta & Radi, 2009). Of particular importance here, NO is a relatively stable
90 radical but reacts with dioxygen and other radicals (Hughes, 2008). Notably, NO reacts with $O_2^{\bullet-}$ to
91 form peroxynitrite ($ONOO^-$), a highly reactive oxidant produced in plant cells undergoing immune
92 responses (Vandelle & Delledonne, 2011). The importance of the interplays between NO and ROS in
93 plant defense has been the subject of particular investigations. Clearly, there is still confusion in
94 understanding their interconnection and reciprocal influences. Indeed, in terms of production NO has
95 been shown to favor or to suppress NADPH oxidase activity (Yun et al. 2011; Rasul et al. 2012) and
96 evidences that ROS also control NO synthesis have been reported (Srivastava et al. 2009).
97 Furthermore, both NO and ROS derived from NADPH oxidase activity were shown to account for HR.
98 However, two distinct processes were proposed. In the first H_2O_2, but not $O_2^{\bullet-}$, was the key ROS
99 effector of HR and played a central role in channeling NO through the cell death pathway
100 (Delledonne et al. 2001; Zago et al. 2006). According to the authors of these studies, $ONOO^-$ was not
101 a mediator of HR. In contrast and according to the situation encountered in animals, in the second
102 process $ONOO^-$ emerged as an essential intermediate of cell death not only during HR but also other
103 physiological processes such as self-incompatible pollination (Alamillo & García-Olmedo, 2001;
104 Serrano et al. 2012). Contrasting roles for NO and ROS in disease resistance have also been
105 highlighted. In particular, Asai and Yoshioka (2009) demonstrated that NO and ROS had opposite
106 effects in *Nicotiana benthamiana* plants infected by *Botrytis cinerea*, NO positively and ROS
107 negatively regulating the basal resistance against the necrotrophic fungal pathogen.

108 Cryptogein is a 10 kDa elicitin produced by the oomycete *Phytophthora cryptogea*. Purified
109 cryptogein causes defense responses in tobacco including HR and SAR against the black shank-
110 causing agent *Phytophthora parasitica* var *nicotianae* as well as against other microbial pathogens
111 (Bonnet et al. 1996). We and other research groups previously reported that cryptogein triggers NO
112 production in leave epidermal tobacco cells and/or in tobacco cell suspensions. The production of NO
113 was assessed using different methods including 4,5 diamino-fluorescein (DAF)-based fluorescence

114 (Foissner et al. 2000; Lamotte et al. 2004; Besson-Bard et al. 2008b), electrochemistry (Besson-Bard
115 et al. 2008b) and an oxidizer column NO detector relying on the ability of CrO_3 to oxidize NO to NO_2,
116 NO_2 being subsequently captured by a Griess reagent trap (Vitecek et al. 2008). All these approaches
117 gave consistent results: NO is produced at the intracellular level within few minutes and diffuses in
118 the extracellular medium and in the gas phase of tobacco cell suspensions elicited by cryptogein. The
119 enzymatic source for NO has not been identified but was shown to be sensitive to mammalian NOS
120 inhibitors (Foissner et al. 2000; Lamotte et al. 2004; Besson-Bard et al. 2008b). Interestingly, the
121 elicitor-induced NO production occurred simultaneously to those of H_2O_2 and $O_2^{\bullet-}$ resulting from the
122 activity of the plasma membrane NADPH oxidase NtRBOHD (Foissner et al. 2000; Simon-Plas et al.
123 2002; Lherminier et al. 2009).

124 Overall, the function of NO in cryptogein signaling is poorly understood but several
125 arguments seem to support a signaling role. Indeed, it has been reported that NO acts as a Ca^{2+}-
126 mobilizing compound contributing to the increase in cytosolic free Ca^{2+} concentration mediated by
127 the elicitor (Lamotte et al. 2004). Supporting an involvement of NO in Ca^{2+} signaling, we recently
128 showed that cryptogein induces the S-nitrosylation of a calmodulin (CaM) tobacco isoform (Astier et
129 al. 2012b; Jeandroz et al. 2013). Besides CaM, other proteins undergoing a fast S-nitrosylation upon
130 cryptogein treatment of tobacco cells were identified. These NO target proteins include NtCDC 48
131 (cell division cycle), a member of the AAA+ ATPase (ATPase associated with various cellular activities)
132 family displaying a chaperone-like activity (Astier et al. 2012b). In animals, CDC48 (named VCP/p97)
133 governs important signaling pathways and, among other functions, helps to deliver protein
134 substrates to the proteasome in quality control pathways (Meyer et al. 2012). A role for NO as an
135 intermediate of cryptogein-triggered cell death has also been proposed as its scavenging reduced the
136 rate of cell death conferred by the elicitor in tobacco cell suspensions (Lamotte et al. 2004). The
137 function of NO in this process has not been elucidated. More generally, our understanding of the
138 mechanisms underlying cryptogein-induced cell death is still faint. Recently, Bourque et al. (2011)
139 demonstrated that NtHD2a and NtHD2b, two redundant isoforms of HDAC (histone deacetylase) of
140 type II, negatively regulate cryptogein-triggered cell death. Impairment of their expression resulted in
141 exacerbated cell death in cell suspension and in the formation of HR-like symptoms in distal leaves.
142 The precise functions of NtHD2a/b in the regulation of cell death, as well as their functional link with
143 NO, are still enigmatic.

144 The possibility that NO interacts with ROS in cryptogein signaling has been previously
145 suggested (Foissner et al. 2000) but not investigated in details. More generally, the interactions
146 between these species have rarely been assessed in a physiological context and, in most of the
147 studies, rely on the use of NO and/or ROS exogenously applied. In the present study, we analyzed the
148 interplays between NO and ROS derived from NtRBOHD in cryptogein signaling in tobacco cell

149 suspensions. Using a combination of pharmacological- and genetic-based approaches, we
150 demonstrated that ROS partly control the production of NO while NO regulates H_2O_2 levels. Further
151 supporting a functional link between NO and ROS, a fast $ONOO^-$ synthesis was detected in elicited-
152 tobacco cells. Furthermore, a transcriptomic analysis led to the identification of cryptogein-induced
153 early genes commonly up-regulated by both NO and ROS but down-regulated by $ONOO^-$. Finally, we
154 provided evidence that NtRBOHD impairment compromises NO involvement in cell death, thus
155 further supporting initial statements that H_2O_2 might channel NO through the cell death pathway
156 (Delledonne et al. 2001; Zago et al. 2006). Taken together, our results provided physiological
157 evidences that NO and ROS derived from NtRBOHD act together in mediating cryptogein signaling.
158

159 **MATERIALS AND METHODS**

160

161 **Cell cultures and treatments**

162 *Nicotiana tabacum* L. cv *Xanthi* were cultivated as previously described (Bourque et al. 2011).
163 Briefly, cells were grown at 25°C on a rotary shaker (150 rpm) and under continuous light (photon
164 flux rate 30-40 $\mu mol.m^{-2}.s^{-1}$) in Chandler's medium (Chandler et al. 1972). Cells were sub-cultured
165 every seven days. Same culture conditions were applied for the distinct cell lines.
166 For elicitor treatments, seven days-old cells were gently filtrated, washed and re-suspended in H10
167 buffer (175 mM mannitol, 0.5 mM $CaCl_2$, 0.5 mM K_2SO_4, 10 mM HEPES, pH 6.0) at a final
168 concentration of 0.1 g/10 mL. Before treatments, cells were equilibrated at 25°C and 150 rpm in the
169 same buffer for 2 or 3 h, depending on the experiments. With the exceptions of fluorescence
170 measurement in which cells were kept in the dark, equilibration were performed under light
171 condition.
172 Cryptogein was purified according to Bourque et al. (2011) and dissolved in water. The NO scavenger
173 cPTIO ((4-carboxyphenyl)-4,4,5,5-tetramethylimidazoline-1-oxyl-3-oxide) was prepared in water and
174 diphenyl iodonium (DPI) in DMSO. DPI and cPTIO were added to the cell suspensions 5 and 10 min
175 before cryptogein, respectively. Control cells were treated with an equal volume of DMSO or water,
176 respectively.
177 The NO donor diethylamine NONOate (DEA/NO) was prepared as previously described (Besson-Bard
178 et al. 2008b). Briefly, a 0.01 M stock solution was prepared daily in NaOH and stored on ice. To
179 initiate the release of NO, an aliquot of the stock solution was dissolved in 100 mM phosphate buffer,
180 pH 7.2, at a final concentration of 2 mM. Few second after its dilution in the phosphate buffer,
181 DEA/NO was applied to the cell suspensions to give a 200 µM final concentration. As a control, cells
182 were treated with an equivalent concentration of diethylamine (DEA) prepared as described for
183 DEA/NO.

184

185 **Chemicals**

186 All basic salts and chemicals were purchased from Sigma-Aldrich (Saint-Louis, USA) unless stated. The
187 CuFL probe was from Strem Chemicals, Inc. (Bischheim, France). cPTIO and DEA/NO were from Alexis
188 Biochemicals (San Diego, USA). Murashige & Skoog medium incl. Nitsch vitamins were from Duchefa
189 Biochemie (Haarlem, The Netherlands). Complete Protease Inhibitors Cocktail was from Roche. γ-
190 [^{32}P] ATP was from Amersham Pharmacia Biotech AB.

191

192 **NO production measurements**

193 The detection of NO using 4,5-diaminofluorescein diacetate (DAF-2DA) was performed
194 according to Lamotte et al. (2004). Filtrated and re-suspended cells were incubated for 1 h with 20
195 µM DAF-2DA. To remove excess of the probe, cells were washed three times with fresh H10 buffer
196 and transferred into 24-well plates (1 mL/well, Costar, Corning Incorporated, Corning, NY, USA). After
197 30 min of incubation, cells were treated with cryptogein, cPTIO, DEA/NO, DPI or DMSO as detailed
198 above. NO production was measured with a spectrofluorometer (Mithras, Berthold Technologies,
199 Germany) using 485 nm excitation and 510 nm emission filters. Fluorescence was expressed as
200 relative fluorescence units.
201 For NO detection with the CuFL probe, filtrated and equilibrated cells were transferred into 24-well
202 plates (1 mL/well). Then, cells were pre-treated or not with cPTIO and exposed 40 min to cryptogein.
203 Five minutes before ending cryptogein treatment, CuFL dissolved in DMSO was added to the cell
204 suspensions with a final concentration of 5 µM. The fluorescence was measured by
205 spectrofluorometry as described for DAF-based fluorescence.
206
207 **H_2O_2 production**
208 ROS production was determined by chemiluminescence as previously described (Pugin et al.
209 1997; Simon-Plas et al. 1997). After application of the treatments, triple aliquots of 250 µL cell
210 suspensions were collected and transferred into vials. Then, cells were automatically supplemented
211 with 300 µL of H50 buffer pH 6.5 (175 mM mannitol, 0.5 mM $CaCl_2$, 0.5 mM K_2SO_4, HEPES 50 mM)
212 containing luminol at a final concentration of 13 µM. Chemiluminescence was measured using a
213 luminometer (Lumat LB9507, Berthold, Bad Wildbad, Germany). The concentration of H_2O_2 was
214 calculated as previously described (Pugin et al. 1997; Simon-Plas et al. 1997) and expressed in
215 nanomoles of H_2O_2 per gram of cells fresh weight.
216
217 **Peroxynitrite production and cellular localization**
218 The production of $ONOO^-$ was measured as followed: equilibrated tobacco cell suspensions
219 kept in the dark were loaded with 5 µM aminophenyl fluorescein (APF) for one hour. After removing
220 excess of the probe, cells were transferred into 24-well plates (1 mL per well) and incubated for 30
221 min before applying cryptogein or the $ONOO^-$ donor SIN-1 (3-morpholinosydnonimine
222 hydrochloride) prepared in a 0.1 M phosphate buffer, pH 7.2.
223 Urate was used as a peroxynitrite scavenger. Urate was dissolved in 1 M NaOH and applied to cells at
224 a final concentration of 1 mM. As controls, cells were supplemented with NaOH at a final
225 concentration of 3.3 mM. A H50 buffer was used to stabilize the pH at 6.0. Fluorescence was
226 measured as described previously for NO detection.

227 In order to determine the cellular localization of $ONOO^-$, seven days-old cells were
228 equilibrated for 2 h in 25°C in the dark under continuous shaking at 150 rpm. Then, cells were treated
229 with 100 nM cryptogein for 0, 20 or 40 min and stained with 15 µM APF for last 5 min of treatment.
230 After three washes with H10 buffer, cells were immediately observed using a confocal laser scanning
231 microscope (Leica TCS 4D; SP2; Leica Microsystems, Heidelberg, Germany) under the 40x NA1 oil
232 immersion objective (HC PL APO CS 40x 0.75-1.25). The light source was a Ar-ArKr (488nm) beam
233 laser and emission of APF fluorescence was pass-filtered between 510-545 nm. Chloroplast
234 autofluorescence was pass-filtered between 665-705 nm. The unspecific background was removed
235 with the median filter of Volocity® 6.1.1 software (PerkinElmer, USA).
236
237 **Analysis of protein kinase activities**
238 Tobacco cells were grounded in liquid nitrogen and 2 mL powder samples were supplemented with
239 250 µL of protein extraction buffer (20 mM Tris-HCl pH 7.5; 2 mM EDTA; 2 mM EGTA; 50 mM -
240 glycerophosphate; 250 mM sucrose; 10 mM Na_3VO_4; 10 mM DTT, 1 mM PMSF; 1x Complete Protease
241 Inhibitors Cocktail) or immunoprecipitation buffer (protein extraction buffer supplemented with 1%
242 Triton X-100 and 150 mM NaCl). The extracts were centrifuged at 14 000 rpm for 30 min at 4°C and
243 supernatants were used for further analysis. The protein concentration was measured using the
244 Protein Assay System described by Bradford (1976) using BSA as the reference for protein
245 concentration.
246 NtOSAK Immunoprecipitation assays: Immunoprecipitation was perfomed as described previously
247 (Kulik et al., 2012) with some minor modifications. Briefly, protein A-agarose beads (15 µL per
248 sample) were washed three times with immunoprecipitation buffer and incubated for 4 hours with
249 antibodies against the C-terminal domain of NtOSAK (24 µg) at 4°C with gentle shaking. After
250 incubation, agarose beads were pelleted by brief centrifugation and washed three times with 1 mL of
251 immunoprecipitation buffer. Protein A-agarose portions with bounded antibodies were added to the
252 protein extracts (200 µg per sample) and incubated for 4 hours at 4°C with gentle shaking. Then,
253 agarose beads-protein complexes were pelleted by brief centrifugation, washed three times with 1
254 mL of immunoprecipitation buffer, two times with 1 mL of 20 mM Tris-HCl pH 7.5 buffer and
255 resuspended in 15 µL of the last buffer. Samples were supplemented with 3x concentrated Laemmli
256 sample buffer (Laemmli, 1970), heated at 95°C for 3 min with vigorous shaking and pelleted by brief
257 centrifugation. The supernatant was analyzed by means of in-gel kinase activity assay
258 (immunocomplex kinase activity assay) using MBP as a substrate.
259 In-gel kinase and Ca^{2+}-dependent and Ca^{2+}-independent kinase activity assays were performed
260 according to Zhang and Klessig (1997) and Szczegielniak et al. (2012). MAPK kinases phosphorylation

261 state was analyzed by the use of commercial Phospho-p44/42 MAPK (Erk1/2) (Thr202/Tyr204)
262 Antibody (Cell Signalling Technology) according to procedure recommended by the manufacturer.
263
264 **Cell death**
265 Cell death was analyzed as previously described (Gauthier et al. 2007) with some
266 modifications. Briefly, seven days-old cells were sub-cultured and incubated for 24 h in Chandler's
267 medium (Chandler et al. 1972). Then, cell suspensions pre-treated or not wit cPTIO were exposed to
268 100 nM cryptogein. A 0.01% final concentration of neutral red was used as a vital dye accumulating
269 in the acidic vacuole. Cells were observed under the light microscope and considered as dead if not
270 accumulating neutral red. The experiment was repeated three times with five hundred cells counted
271 for each assay.
272
273 **Microarray analysis**
274 The transcriptomic analysis was performed on wild type tobacco cells. For this purpose, cells
275 pre-incubated or not with 500 µM cPTIO were treated with 100 nM cryptogein for 30 min. Samples
276 were collected from three independent batches and three independent experiments were
277 performed. Filtrated cells were immediately frozen in liquid nitrogen, then RNA were extracted with
278 RNeasy Plant Mini Kit (Qiagen, Courtabeuf, France) and purity and concentrations estimated using
279 Nanodrop1000 (Thermo Fisher Scientific, Waltham, USA) and Agilent 2100 Bioanalyzer (Agilent
280 Technologies, Santa Clara, USA). RNA samples were hybridized on a 4x44K slides Tobacco Gene
281 Expression Microarray, manufactured by Agilent Technologies (Santa Clara, USA), content sourced
282 from TIGR Release 3, Unigene Build 11, TIGR PlantTA Release 5. The microarray slides contained
283 43 804 different tobacco test sequences and 1417 control sequences. Samples single color labeling
284 (Low Input Quick Amp Labelling Kit, one color), hybridization (Microarray hybridization oven, Agilent)
285 scanning (High resolution Microarray scanner G2505C, Agilent) and data extraction (Feature
286 Extraction V10 software) were done by the Biopuce GenoToul Plateform
287 (https://genomique.genotoul.fr/). The quintile normalization was done with GeneSpring. Ink 12.0
288 software (Agilent). To investigate the homogeneity between biological replicates, hierarchical
289 clustering and principal component analysis were performed using the R Gui open-source software
290 (R: A Language and Environment for Statistical Computing. R Core Team. R Foundation for Statistical
291 Computing. Vienna, Austria. 2013. http://www.R-project.org). Differential expression between
292 groups was assessed thanks to moderated paired t-test implemented in Limma package of
293 Bioconductor (Smyth, 2004): genes were selected by Fold Change > 4 and False Discovery Rate (FDR)
294 adjusted p-values < 0.01 taking into account multiple testing using Benjamini and Hochberg (1995)
295 correction. Annotation implementation was performed for the best matched *Nicotiana tabacum* SGN

296 mRNA ESTs homological to microarray sequences after translation to protein sequences. Functional
297 analysis of genes with annotations to *Arabidopsis thaliana* was done with MapMan 3.5.1R2 free
298 software (Max Planck Institute, Munich, Germany).
299
300 **qRT-PCR analyses**
301 RNAs were extracted from liquid nitrogen-preserved cells using Trizol reagent according to
302 the manufacturer's instructions (Invitrogen, Paisley, UK). Genomic DNA contamination was removed
303 by treatment with DNase 1. The reverse transcription was performed on 500 ng of pure RNA samples
304 using the ImpromIITM Reverse Transcriptase kit (Promega) with anchored oligo (dT15) (Promega)
305 and 0.4 mM deoxynucleotide triphosphates. The resulting cDNAs were diluted ten times with water
306 and 1 µl of each cDNA sample was assayed by qPCR in a Abi Prism 7900HT Sequence Detection
307 System (Applied Biosystems, Foster City, USA) using cGoTaq® qPCR Master Mix (Promega).
308 Expression levels were calculated relatively to the housekeeping genes *Ntubc2, L25* and *EF-1α*
309 (Schmidt & Delaney, 2010) using the relative standard curve method. For each sample, target
310 quantity of the gene of interest was determined by interpolating the value from the standard curve
311 made from a cDNA pool which enables to take into consideration the efficiency of amplification. The
312 value was then divided by the target quantity of the housekeeping gene.
313 To design primers for verifying the expression of the sequences used on microarray chips, the
314 homolog ESTs were found on the http://solgenomics.net/ webpage by the search for *Nicotiana*
315 *tabacum* SGN mRNA. All obtained sequences were aligned and contigs of sequences were prepared
316 with Vector NTI Advance 11 (Life Technologies, Carlsbad, USA). Primers were designed as suitable to
317 detect every sequence.
318 Primer sequences were as follows: Ntubc2-fw: 5'-CTGGACAGCAGACTGACATC -3'; Ntubc2-rev: 5'-
319 CAGGATAATTTGCTGTAACAGATTA-3'; L25-fw: 5'-CCCCTCACCACAGAGTCTGC-3'; L25-rev: 5'-
320 AAGGGTGTTGTTGTCCTCAATCTT-3'; EF-1α-fw: 5'-TGAGATGCACCACGAAGCTC-3'; EF-1α-rev: 5'-
321 CCAACATTGTCACCAGGAAGTG-3';
322 A_95_P128872-fw: 5'-CTCAGTGCGTTAACGGAACAAGTTCAACAAG-3'; A_95_P128872-rev: 5'-
323 CCAGCATTCAATACAAACAAGATGATTCCACATGTC-3'; A_95_P138477-fw: 5'-
324 CGGATTCCGACGCCGAAACAAC-3'; A_95_P138477-rev: 5'- CATTGTTCGCCGAAATTACGGATCGATTC-3';
325 A_95_P121687-fw: 5'- CAGAAATGGACGGCGGGTTTAACAATG-3'; A_95_P121687-rev: 5'-
326 CGAATGTATTTCGAGCGCTCTCCGC-3'; A_95_P139122-fw: 5'-
327 GTATACAGAAATGGACGGCGGGTTTAACAATG-3'; A_95_P139122-rev: 5'-
328 CGCCGTTGAGAAGAAGGCGATAATCTTC-3'; A_95_P082790-fw: 5'- AACTGGGTCTGAGTATTGATTG-3';
329 A_95_P082790-rev: 5'- CCCTGTACATAATACCACCCTAA-3'; NtrbohD-fw: 5'-

330 CCAAAGATTGGTACAAGAGAACGACATGG-3'; NtrbohD-rev: 5'-
331 CAGTTTTAAGTTGTCTGGTCCAATCACCAAG-3'.
332
333 **Statistical analysis**
334 Significant differences between treatments were analyzed with Sigma Plot for Windows
335 Version 11.0 (Systat Software Inc., Chicago, USA) by ANOVA test followed by stepwise multiple
336 comparison procedure the Student-Neuman-Keuls (SNK) method ($P < 0.05$).
337

338 **RESULTS**

339

340 **Nitric Oxide and ROS production: analysis of mutual regulation**

341

342 NO production in tobacco cells exposed to cryptogein was monitored using the NO-sensitive
343 fluorophore DAF-2DA as well as with the CuFL fluorescent probe. The DAF-2DA method is indirect
344 and based on the measurement of RNS derived from NO autoxidation that nitrosate DAF-2 to yield to
345 the fluorescent DAF-2 triazole (DAF-2T; Jourd'heuil, 2002). The CuFL dye consists in a fluorescein-
346 based ligand (FL) complexed with Cu(II). NO induces the reduction of Cu(II) to Cu(I), forming NO^+,
347 which in turn nitrosates the ligand, thus giving the fluorescent FL-NO compound. CuFL allows the
348 direct detection of NO with nanomolar sensitivity (Lim et al. 2006) and has been successfully used for
349 NO detection in plants (Horchani et al. 2011; Rasul et al. 2012).
350 As we previously reported (Lamotte et al. 2004; Besson-Bard et al. 2008b), cryptogein triggered an
351 increase in DAF-2T fluorescence which occurred within 10 min of treatment and was maintained for
352 at least 80 min (Fig. 1A). The cryptogein-induced rise in fluorescence was almost completely
353 suppressed by the membrane-permeable NO scavenger cPTIO. Although we cannot exclude the
354 possibility that cPTIO might exert unspecific effects, its ability to act as a powerful NO scavenger has
355 been widely reported (Foissner et al., 2000). Similarly, cryptogein treatment led to a significant
356 increase of CuFL fluorescence (Supporting Information Fig. S1A). Here too, this process was deeply
357 reduced by cPTIO. The effect of cPTIO, as well as the consistent results provided by the DAF-2DA and
358 CuFL methods, further confirmed the ability of cryptogein to induce NO synthesis in tobacco cells.
359 To investigate the potential interplays between NO and ROS, in a first series of experiments
360 NO synthesis was examined in gp15 cell suspensions. The gp15 cells are transformed with antisense
361 constructs of the NADPH oxidase NtRBOHD, the major enzymatic source for H_2O_2 in cryptogein
362 signaling (Simon-Plas et al. 2002). As shown in Fig. 1B, cryptogein mediated a fast and transient H_2O_2
363 production in wild-type (wt) tobacco cells which, as expected, was not observed in gp15 cells. Of
364 interest, both H_2O_2 and NO production occurred within few minutes (Fig. 1A and 1B). When NO
365 production was assessed in gp15 cell suspensions, compared to wt cells a reduction of nearly 40%
366 was observed, whatever the dye used for NO detection (Fig. 1C and Supporting Information S1B).
367 This reduction was not due to a lower permeability of gp15 cells to the probe (Fig. S2A). This data
368 suggested that ROS derived from NtRBOHD activity could partly control NO production. To further
369 support this assumption, the effect of the commonly used NADPH oxidase inhibitor
370 diphenyliodonium (DPI) was also tested. DPI is a general inhibitor of flavine oxidoreductases
371 previously shown to inhibit plant NADPH oxidases (Pugin *et al*., 1997). DPI, which severely blocked
372 the cryptogein-induced H_2O_2 synthesis (Supporting Information Fig. S3), suppressed NO synthesis by

373 40%. Although DPI might affect flavine oxidoreductases distinct than NtRBOHD, both the genetic and
374 pharmacological impairment of H_2O_2 production partly and similarly impacted the elicitor-triggered
375 NO production.

376 To better assess the cross-talk operating between NO and H_2O_2, the incidence of NO on H_2O_2
377 synthesis was also analyzed. For this purpose, H_2O_2 production was measured in tobacco cells
378 exposed to cryptogein in the presence of the NO scavenger cPTIO. Scavenging of NO significantly
379 increased the level of H_2O_2 by a 1.5 fold (Fig. 2), suggesting that NO influenced the rate of H_2O_2 in
380 tobacco cells facing cryptogein treatment. Besides reinforcing the assumption that NO and H_2O_2 are
381 closely linked, this result also indicated that cPTIO did not scavenge H_2O_2 as previously reported
382 (Foissner et al. 2000).

383 To complete this work, the interplay between NO and H_2O_2 was also studied in CL5 cell
384 suspensions. This stable silenced cell line is impaired in the expression of NtHD2a and NtHD2b, two
385 redundant isoforms of HDAC acting as negative regulators of cryptogein-induced cell death (Bourque
386 et al. 2011). Interestingly, compared to control cells, following cryptogein treatment the CL5 cells
387 displayed a low production of H_2O_2 picking at 20 min (Fig. 3A). The cryptogein-induced NO synthesis
388 was also significantly affected in the CL5 cell line, 50% to 60% of inhibition being observed depending
389 on the method used to assess NO production (Supporting Information Fig. S1C and Fig. 3B,
390 respectively). Here too, we checked that this reduction was not caused by a lower permeability of
391 CL5 cells to the probe (Supporting Information Fig. S2B). Because ROS derived from NtRBOHD
392 appeared to partly control NO production (Fig. 1), the lower NO synthesis measured in CL5 cells was
393 expected. To further explore the functional relationship between NO and ROS, we also examined the
394 level of NtRBOHD transcript in CL5 cells. We found that the accumulation of the corresponding mRNA
395 was not statistically different between control and CL5 lines (data not shown), ruling out the
396 hypothesis that the low H_2O_2 production observed in the CL5 line could be related to an impaired
397 expression of *NtRBOHD*.

398 Collectively, data from these experiments highlight the occurrence of a functional link
399 between NO and NtRBOHD-derived ROS in tobacco cells elicited by cryptogein. NO production
400 appears to be partly dependent on ROS and NO impacts the level of H_2O_2.

401

402 **Cryptogein induces a production of peroxynitrite**

403

404 We next investigated whether cryptogein could induce a production of $ONOO^-$. The
405 generation of $ONOO^-$ results from the coupling reaction of $O_2^{\bullet-}$ with NO in its radical form ($NO^\bullet$;
406 Ferrer-Sueta & Radi, 2009). Supporting this initiative, as showed above the productions of NO and
407 ROS derived from NtRBOHD activity occur simultaneously. For this purpose, we used the fluorescent

408 probe aminophenyl fluorescein (APF). APF reacts preferentially with $ONOO^-$ and was successfully
409 used to detect this reactive species in plants (Saito et al. 2006; Gaupels et al. 2011b; Begara-Morales
410 et al. 2013). However, it also shows reactions with hypochlorite (^-OCl) and hydroxyl radical ($^{\bullet}OH$;
411 Setsukinai et al. 2003). To check the efficiency of this probe as an $ONOO^-$ indicator, APF-loaded
412 tobacco cells were first treated with the $ONOO^-$ donor SIN-1 (Fig. 4A). A significant increase of APF
413 fluorescence reaching a plateau after 2 hours was detected in SIN-1-treated cells. To further confirm
414 that the observed increase in APF fluorescence was caused by $ONOO^-$, a similar experiment was
415 performed in presence of the ONOO− scavenger urate as previously reported (Gaupels et al. 2011b).
416 Urate strongly suppressed SIN-1-induced rise of fluorescence, providing evidence that APF is a
417 reliable tool to investigate $ONOO^-$ generation in tobacco cell suspensions. It should be noticed that
418 because urate was dissolved in NaOH, in all the assays cells were supplemented with an equivalent
419 volume of NaOH at a final concentration of 3.3 mM, the pH of the culture media being stabilized at 6.
420 In this condition, the control cells showed a rise of fluorescence during the experiment (Fig. 4A and
421 4C).
422 Next, we applied a similar approach in cryptogein-treated cells. As shown Fig. 4B and 4E, the
423 elicitor triggered a fast and pronounced rise in APF fluorescence which mainly occurred in
424 chloroplasts and, to a lower extend, in the nucleus and along the plasma membrane. This increase
425 was partially sensitive to urate (Fig. 4C), supporting the assumption that cryptogein triggered a
426 production of $ONOO^-$. The fact that $ONOO^-$ generation results from the reaction between $O_2^{\bullet-}$ and
427 NO also pushed us to check its production in gp15 and CL5 cells. As expected, depletion of NtRBOHD
428 expression and, therefore, of $O_2^{\bullet-}$ production abrogated the elicitor-mediated increase of APF
429 fluorescence (Fig. 4B and 4E). Similarly, only a slight rise in APF fluorescence was measured in
430 cryptogein-treated CL5 cells producing reduced levels of ROS and NO (Fig. 4D). Taken together, these
431 data strongly suggest that a production of $ONOO^-$ occurs in tobacco cells exposed to cryptogein.
432
433 **NtRBOHD-derived ROS regulate the activity of NtOSAK, a member of the SnRK2 protein kinase**
434 **family**
435
436 Previous studies highlighted the ability of cryptogein to induce activation of distinct protein
437 kinases including Ca^{2+}-dependent protein kinases and mitogen-activated protein kinases (MAPK)
438 including WIPK (wound-induced protein kinase) and SIPK (salicylic acid-induced protein kinase)
439 (Klessig et al., 2000; Dahan et al., 2009). In order to provide a better view of the signaling functions of
440 NO and ROS, their incidence on the regulation of cryptogein-induced protein kinases (PK) was
441 examined. Therefore, protein extracts from wild type tobacco cells treated with cryptogein in the
442 presence or not of cPTIO or from gp15 cells exposed to the elicitor were analyzed for PK activities by

443 in-gel kinase assays with MPB (myelin basic protein) as a substrate or by the use of commercial
444 antibodies raised against phosphorylated residues of MAPKs.
445 Compared to wild type cells exposed to cryptogein, activities of the elicitor-induced MAPKs,
446 Ca^{2+}-dependent and -independent kinases were not significantly changed in cells pre-treated with
447 the NO scavenger cPTIO or in gp15 cells (data not shown). These data indicate that neither NO or
448 ROS derived from NtRBOHD contribute to the activities of these PK in cryptogein signaling. To
449 complete this work, we next analyzed the putative involvement of NtOSAK (*Nicotiana tabacum*
450 Osmotic Stress-Activated protein Kinase), a tobacco serine/threonine protein kinase belonging to the
451 SNF1 (Sucrose Non-Fermenting 1)-Related Kinases type 2 (SnRK2) family (Burza et al., 2006). Previous
452 studies have shown that NtOSAK is rapidly and transiently activated in response to salt and osmotic
453 stresses as well as in response to the toxic metal cadmium (Cd, Burza et al., 2006; Kulik et al., 2012).
454 Further supporting our interest for this PK, NO donors, H_2O_2 as well as NO and/or ROS endogenously
455 produced in response to salt and Cd were shown to contribute to NtOSAK activation (Wawer et al.,
456 2010; Kulik et al., 2012). Based on these findings, we first investigated whether cryprogein could
457 trigger the activation of NtOSAK. To check this possibility, proteins extracts from cryptogein-treated
458 wild type tobacco cells were analyzed by immunocomplex-kinase activity assays using antibodies
459 raised against NtOSAK. As shown in Fig. 5, the elicitor triggered a transient activation of NtOSAK, the
460 maximum of activity being observed after 3 and 6 hours of elicitation. Next, NtOSAK activity was
461 assessed in cryptogein-treated wild type cells in presence of cPTIO as well as in gp15 cells. The NO
462 scavenger cPTIO did not affect the activation of this PK (data not shown). In gp15 cells, a slight
463 activity of NtOSAK was already detected before cryptogein addition to the cell suspensions.
464 Importantly, the intensity of its activity was exacerbated during the course of cryptogein treatment
465 while its kinetic of activation was similar to those observed in wild type cells (Fig. 5). This observation
466 suggested that the ROS derived from NtRBOHD might negatively regulate the intensity of NtOSAK
467 activity.
468
469 **Identification of NO-regulated genes during cryptogein treatment**
470
471 To further study the interplays between NO and ROS, we checked whether NO and ROS could
472 regulate the expression of common genes. First we looked for genes modulated by cryptogein
473 through a NO-dependent process. An expression profiling of tobacco cell suspensions was performed
474 using a tobacco gene expression microarray (Agilent Technologies) consisting of about 44,000 probes
475 with an average length of 60 nucleotides. For this purpose, wt tobacco cell suspensions pre-treated
476 or not for 10 min with the NO scavenger cPTIO were elicited with cryptogein for 30 min. Genes which

477 corresponding transcripts showed a fold change higher than 4 in response to cryptogein treatment,
478 but lower than 4 in cells co-treated with the elicitor and cPTIO, were selected as NO target genes.
479 The microarray analysis revealed that compared to non-elicited control cells, 135 microarray
480 probes displayed significant increased labeling with a fold change > 4 after 30 min of cryptogein
481 treatment. In contrast, cryptogein did not trigger the down-regulation of genes. Using annotation
482 tools, 71 of the 135 probes were linked to *Arabidopsis thaliana* genes (data not shown). Interestingly,
483 in tobacco cells co-treated with cPTIO and cryptogein, among these 135 probes, 35 showed an
484 altered expression, that is a fold change < 4. Fifteen of them matched to *A. thaliana* genes and,
485 according to our selective criterion, were defined as NO target genes. The list of these genes, as well
486 as their functional classes, are provided in Table 1. About 40 % of these genes encode proteins
487 involved in signaling, notably protein kinases including CIPK 11, a member of the CIPK (Calcineurin B-
488 like (CBL) Interacting Protein Kinase) family. CIPKs are related to yeast sucrose-non-fermenting
489 protein kinases and animal AMP-activated protein kinases. Upon their activation by the Ca^{2+} sensors
490 CBLs, CIPKs phosphorylate downstream targets and, consequently, mediate Ca^{2+} signaling (DeFalco et
491 al. 2010). In *A. thaliana*, CIPK11 was shown to inhibit the activity of the plasma membrane proton
492 pump H^+-ATPase AHA2 by abolishing the binding of 14-3-3 protein through a phosphorylation-
493 dependent process (Fuglsang et al. 2007). According to the authors, CIPK11 is a key actor of the Ca^{2+}-
494 dependent regulation of plasma membrane H^+-ATPase activity and extracellular acidification. Further
495 supporting a link between NO and Ca^{2+} signaling, we identified two genes encoding CaM-binding
496 protein including the tobacco orthologue of the *A. thaliana* transcription factor EDA39 (Embryo sac
497 Development Arrested 39) previously shown to be induced by chitin and by the oomycete
498 *Peronospora parasitica* (Eulgem et al. 2004; Libault et al. 2007). More generally, the identification of
499 genes related to Ca^{2+} signaling fits well with our previous findings showing that Ca^{2+} and NO work
500 together in mediating responses to pathogenic microorganisms and elicitors including cryptogein
501 (Courtois et al. 2008; Rasul et al. 2012; Jeandroz et al. 2013). *ZAT6* is another signaling-related gene
502 of interest. In *A. thaliana*, it encodes a C2H2 zinc finger transcription factor previously shown to be
503 inducible by chitin (Libault et al. 2007) and involved in the regulation of salt and osmotic stress
504 responses (Liu et al. 2013), two stresses promoting NO synthesis (Gould et al. 2003). Besides
505 signaling, three genes encoding proteins putatively involved in protein degradation were also found
506 as NO-responsive genes. The *A. thaliana* orthologues correspond to PUB26, RHC2A and DUF1
507 displaying ubiquitin-ligase activities. This latter was shown to be involved in ABA and, once again, in
508 chitin signaling (Libault et al. 2007; Kim et al. 2012). The other NO-dependent genes encode proteins
509 related to hormone metabolism, vesicle transport and development. Intriguingly, only one NO-
510 dependent gene, the tobacco orthologue of NUDX2, encodes a protein related to oxidative stress.

511 NUDX2 was indeed reported as being an ADP-ribose pyrophosphatase involved in tolerance to
512 oxidative stress in *A. thaliana* (Ogawa et al. 2009).
513 Next, we checked whether the NO-dependent cryptogein-induced genes could be also
514 regulated through ROS derived from NtRBOHD. For this purpose, we measured their level of
515 expression by quantitative real-time PCR in wt and gp15 cells exposed to cryptogein for 30 min.
516 Among the 15 NO-dependent genes, 4 were found as being both NO- and ROS-dependent including
517 the tobacco orthologues of *CIPK11*, *RHC2A*, *PUB26* and *DUF1* (Table 2). Indeed, the cryptogein-
518 induced accumulations of the corresponding transcripts were all found to be significantly reduced in
519 cPTIO-treated cells as well as in gp15 cells. In contrast and as an example, expression of the tobacco
520 orthologue of *ZAT6* encoding a transcription factor appeared to be NO-dependent but ROS
521 independent as the accumulation of the corresponding transcript was impaired in cPTIO-treated cells
522 and unmodified in gp15 cells. Taken together, these results confirm the data described above
523 indicating that part of the cryptogein-triggered NO production (around 40%) is under the control of
524 NtRBOHD-derived species. Therefore, the NO target genes might be regulated through a ROS-
525 dependent but also a ROS-independent pathway.
526 Since the expression of the tobacco orthologues of *CIPK11*, *RHC2A*, *PUB26* and *DUF1*
527 appeared to be under the control of both NO and ROS in response to cryptogein treatment, we
528 investigated whether the accumulation of the corresponding transcripts could be also regulated
529 through $ONOO^-$ (Fig. 6). When tobacco cell suspensions were pretreated with the $ONOO^-$ scavenger
530 urate, the cryptogein-induced accumulation of the transcripts of interest was significantly increased.
531 This data suggested that $ONOO^-$ mitigates the level of expression of these genes.
532
533 **Analysis of NO and ROS involvement in cryptogein-triggered cell death**
534
535 Nitric oxide and ROS are commonly designed as cell death mediators (Yoshioka et al. 2011).
536 In the present study, we analyzed their respective involvement in the cell death triggered by
537 cryptogein. As previously reported (Bourque et al. 2011), in wt tobacco cell suspensions cryptogein
538 induced a significant cell death reaching 60% after 24 hours (Fig. 7). This percent was reduced to 13%
539 in cells co-treated with the NO scavenger cPTIO, highlighting the involvement of NO, or NO-derived
540 species, in the mechanisms leading to cell death. In gp15 cells, the percent of cell death mediated by
541 the elicitor was reduced as compared to wt cells and reached only 36%, suggesting that ROS also play
542 a role in this process. To better evaluate the contribution of NO in the cell death occurring in gp15
543 cells in response cryptogein treatment, we checked the effects of NO scavenging. Remarkably, cPTIO
544 did not impact the level of cell death triggered by the elicitor in gp15 cells.

545 To complete this study, a similar analysis was performed in the CL5 cell line. As stated above,
546 this line does not express NtHD2a and NtHD2b, two HDACs isoforms acting as repressors of
547 cryptogein-induced cell death (Bourque et al. 2011). Furthermore, as described in Fig. 3 and S1, this
548 line displayed a reduced production of NO and a low level of H_2O_2 when challenged by cryptogein. As
549 shown in Fig. 7B, compared to control cells, the CL5 cells displayed a higher rate of cell death in
550 response to cryptogein, confirming a role for NtHD2a and NtHD2b as negative regulators of cell
551 death. This data also indicates that in contrary to gp15 cells, the reduced production of H_2O_2
552 observed in CL5 cells was not correlated to a lower occurrence of cell death. Regarding the incidence
553 of NO on cryptogein-induced cell death in the CL5 line, its scavenging reduced by about 35% the rate
554 of cell death.
555

556 **DISCUSSION**

557

558 In this work we investigated the interplays operating between NO and ROS derived from
559 NtRBOHD activity in tobacco cells elicited by cryptogein. Our results indicated that these species
560 modulate their respective production/levels, interact by forming peroxynitrite and influence the rate
561 of cell death. Furthermore, NO appeared to function independently or in cooperation with ROS to
562 regulate the expression of genes related to signaling and protein degradation amongst other
563 functions.

564 Deficiency of ROS, through the impairment of NtRBOHD expression in gp15 cells or using DPI,
565 resulted in decreasing NO production by about 40%. Accordingly, the cryptogein-mediated NO
566 synthesis was partly suppressed in CL5 cells producing a low level of ROS. These data highlighted a
567 key role for ROS in modulating NO production. Several studies also provided evidence that ROS act
568 upstream of NO production. For instance, Srivastava et al. (2009) reported that NO synthesis occurs
569 downstream of ROS production in *Pisum sativum* guard cells treated with chitosan. Similarly, using
570 the NADPH oxidase-deficient double mutant *AtrbohD/F*, Bright et al. (2006) demonstrated that
571 endogenous H_2O_2 production is required for ABA-induced NO synthesis in *A. thaliana* guard cells. In
572 contrast, mechanisms in which NO promotes ROS production were also described. For example, in *A.*
573 *thaliana* leaves exposed to oligogalacturonides, NO was shown to positively regulate AtRBOHD-
574 mediated ROS synthesis (Rasul et al. 2012). In our study, the situation is rather complex as NO also
575 controls ROS levels. Indeed, we observed that the scavenging of NO enhanced by a 1.5 fold the
576 concentration of H_2O_2 in tobacco-elicited cells. Therefore, a bidirectional cross-talk occurs between
577 both species: ROS appear as a step in the signaling cascade leading to NO production which further
578 modulates the rate of H_2O_2.

579 The conclusion stated above raises the question of the mechanisms underlying this cross-
580 regulation. Regarding the ROS-dependence of NO production, it has been previously shown that the
581 synthesis of NO mediated by cryptogein requires Ca^{2+} influx from the extracellular space (Lamotte et
582 al. 2004). As H_2O_2 produced by NtRBOHD was assumed to contribute to this influx by promoting the
583 activation of putative plasma membrane Ca^{2+}-permeable channels (Lecourieux et al. 2002), the
584 resulting rise of cytosolic Ca^{2+} could constitute a relay connecting H_2O_2 to NO. Concerning the
585 regulation of ROS by NO, at least two scenarios might be envisaged. First, the enhancement of H_2O_2
586 concentration observed in cPTIO-treated cells following cryptogein exposure could reflect a negative
587 regulation of NtRBOHD by NO. Supporting this hypothesis, Yun et al. (2011) found that NO abolishes
588 AtRBHOD activity through S-nitrosylation of a critical Cys residue. This process destabilizes FAD or
589 precludes its binding to the enzyme. According to the authors, S-nitrosylation of NtRBOHD serves to
590 control ROS generation in cells facing pathogen attack and curbs their deleterious effects leading

591 notably to excessive cell death. In a recent proteome-wide analysis aimed at identifying S-
592 nitrosylated proteins in cryptogein signaling (Astier et al. 2012b), we were not able to identify NADPH
593 oxidases as NO protein targets, thus questioning the possibility that NO could mitigate ROS
594 production through NtRBOHD S-nitrosylation. However, a note of caution is required as the method
595 used to selectively identify S-nitrosylated proteins is poorly efficient at targeting transmembrane
596 proteins. Furthermore, NtROBOHD is a low abundant protein, reinforcing the difficulty in identifying
597 this protein. Second, the enhanced H_2O_2 level observed in cPTIO-preated cells could be explained by
598 a coupling reaction of NO and $O_2^{\bullet-}$ leading to $ONOO^-$ formation. Indeed, if such mechanism occurs,
599 the scavenging of NO by cPTIO might enhance $O_2^{\bullet-}$ availability and, consequently, H_2O_2
600 concentration. Supporting this hypothesis, we demonstrated that cryptogein triggered a fast increase
601 of APF fluorescence. This increase was markedly reduced in presence of the $ONOO^-$ scavenger urate
602 and severely suppressed in gp15 cells impaired in NtRBOHD expression, confirming the assumption
603 that APF fluorescence is indicative of $ONOO^-$ synthesis. More generally, the formation of $ONOO^-$ is
604 very fast and the corresponding reaction between NO and $O_2^{\bullet-}$ competes with other routes that
605 consume $O_2^{\bullet-}$, notably the route involving SOD, its ultimate scavengers (Ferrer-Sueta & Radi, 2009).
606 At least two factors promote its formation: the temporal occurrence of NO and $O_2^{\bullet-}$ and the location
607 of NO and $O_2^{\bullet-}$. Both criteria are fulfilled in the case of cryptogein signaling. Indeed, NO and ROS are
608 produced simultaneously. Furthermore, similarly to NO (Foissner *et al.*, 2000; Fig. S4), $ONOO^-$ was
609 localized in the plastids, slightly in the nucleus and probably in the cytosol along the plasma
610 membrane. Besides this work, several studies provided mounting evidence that $ONOO^-$ is generated
611 in plant cells undergoing immune responses (reviewed by Vandelle & Delledonne, 2011). For
612 instance, in their pioneer work, Saito et al. (2006) measured a fast $ONOO^-$ production in tobacco BY-
613 2 cells exposed to INF1, the main elicitin secreted by the late blight pathogen *Phytophthora infestans*.
614 Here too, $ONOO^-$ synthesis was detected using APF and the resulting increase of fluorescence was
615 suppressed by urate. More recently, a urate-sensitive $ONOO^-$ accumulation was measured in *A.*
616 *thaliana* leaves challenged with the avirulent pathogen *Pseudomonas syring*ae pv tomato carrying
617 the *AvrB* gene (Gaupels et al. 2011b). The involvement of $ONOO^-$ in the plant immune response was
618 further supported by the characterization/identification of proteins regulated by tyrosine nitration, a
619 post-translation protein modification mediated by $ONOO^-$ (Saito et al. 2006; Romero-Puertas et al.
620 2007; Cecconi et al. 2009). According to Gaupels et al. (2011b), tyrosine nitration might represent a
621 major mean by which cells facing pathogen attack mediate the NO/ROS signal.
622
623 To investigate the incidence of NO and/or ROS on cryptogein signaling, we analyzed their
624 respective involvement in cryptogein-induced PK activities and genes expression. The possibility that
625 NO or ROS produced in the context of defense responses regulate the activity of PK has been

626 previously reported. These PKs include MAPK and CDPK (see for instance Grant et al., 2000; Yoshioka
627 et al., 2011) but not SnRK2s. Through in gel kinase activity assays and western-blotting based
628 approaches, we found that neither NO nor ROS controlled the activity of MAPK and Ca^{2+}-
629 dependent/independent PK (data not shown). In contrast, ROS derived from NtRBOHD negatively
630 regulated the intensity of the SnRK2 PK NtOSAK. Supporting this assumption, NtOSAK activity was
631 remarkably increased in gp15 cells elicited by cryptogein as compared to wild type cells. In contrast,
632 its kinetic of activation was similar in both genotypes. Interestingly, the NO scavenger cPTIO did not
633 impact its kinetic as well as its intensity of activity in cryptogein-treated wild type cells. Collectively,
634 these data highlight a specific action of ROS and not NO on cryptogein-induced NtOSAK activity.
635 Importantly, they differ from previous findings indicating that the activity of this PK is up-regulated
636 by NO and/or ROS in tobacco cells challenged by Cd or salt stresses (Wawer et al., 2010; Kulik et al.,
637 2012). Therefore, although our study confirms the regulation of NtOSAK by ROS, it points out a
638 distinct regulation of this PK by NO and/or ROS according the cellular conditions. More generally,
639 although a role for SnRK2.4, the closest homolog of NtOSAK in *A. thaliana*, in the regulation of plant
640 tolerance to cadmium has been reported (Kulik et al., 2012), its function in plant defense remains to
641 be determined.

642 The microarray analysis allowed the identification of 15 early-modulated genes, which
643 induction by cryptogein was suppressed by cPTIO. Because cPTIO reduced the elicitor-induced NO
644 synthesis by almost 70% (Fig. 1), these genes were defined as NO target genes. Accordingly, several
645 *A. thaliana* orthologues of these genes were also found as being induced by NO (*At1G21380*,
646 *At2G41380*, *At3G46620*, *At5g04340* and *At5G47070*; Parani et al. 2004; Ahlfors et al. 2009; Besson-
647 Bard et al. 2009). Furthermore, the tobacco genes orthologues of *At3G46620* and *At5G47070*
648 encoding a C3HC4-type RING finger protein and a putative protein kinase, respectively, were shown
649 to be modulated in tobacco leaves infiltrated with the NO donor sodium nitroprusside (Zago et al.
650 2006). Interestingly, a significant part of these genes encode proteins related to signaling. This
651 observation confirms our previous conclusion, as well as those of other teams, that NO displays a
652 signaling function in plant immunity (see for instance Besson-Bard et al. 2008a; Gaupels et al. 2011b;
653 Bellin et al. 2013; Skelly & Loake, 2013). The identification of the tobacco orthologue of *CIPK11*, a
654 gene encoding CBL-interacting protein kinase in *A. thaliana*, is of particular interest. Indeed, as
655 described in the results section, CIPK11 is a critical negative regulator of the plasma membrane H^+-
656 ATPase that controls extracellular acidification (Fuglsang et al. 2007). According to these authors, a
657 negative regulation of the plasma membrane H^+-ATPase by CIPK11 might be an advantage under
658 conditions where H^+-ATPase activity has to be rapidly down-regulated, notably in response to fungal
659 elicitors inducing plasma membrane depolarization and cytoplasmic acidification such as cryptogein
660 (Pugin et al. 1997; Gauthier et al. 2007). Whether the NO-dependent induction of the tobacco

661 orthologue of CIPK11 is related to the regulation of plasma membrane H^+-ATPase in cryptogein-
662 induced effects remains to be investigated but warrants attention. Another NO-dependent gene of
663 interest is the tobacco orthologue of *AtNUDX2*. The corresponding protein displays ADP-ribose
664 pyrophosphatase activity (Ogawa et al. 2005). In animal cells, free ADP-ribose is a highly reactive
665 compound molecule that causes the nonenzymatic mono-ADP-ribosylation of proteins and
666 contributes to the activation of apoptosis during oxidative stress (Perraud et al. 2005). Ogawa et al.
667 (2009) reported that the overexpression of *AtNUDX2* in *A. thaliana* increased tolerance to oxidative
668 stress caused by salinity or paraquat. This tolerance was correlated to the ability of the enzyme to
669 metabolize potentially toxic ADP-ribose to AMP and ribose 5-phosphate. Here too, understanding the
670 physiological significance of *NUDX2* expression in tobacco, as well as its regulation by NO, will require
671 further investigation.

672 Amongst the NO-dependent genes modulated in response to cryptogein, 4 (the tobacco
673 orthologues of *CIPK11*, *RHC2A*, *PUB26* and *DUF1*) were also found as being down-regulated in gp15
674 cells treated with the elicitor. This finding indicates that NO drives specific but also mutual signaling
675 pathway(s) shared with ROS derived from NtRBOHD activity. A similar conclusion has been raised by
676 Zago et al. (2006) who demonstrated that in tobacco NO and H_2O_2 act either individually or in
677 partnership in regulating gene expression. Further supporting the involvement of both NO and ROS
678 in regulating the expression of *CIPK11*, *RHC2A*, *PUB26* and *DUF1*, we observed that the scavenging of
679 $ONOO^-$ significantly increased the cryptogein-triggered accumulation of the corresponding
680 transcripts. This data further support the hypothesis that $ONOO^-$ formation mitigates the effects of
681 ROS and NO. It is noteworthy that 3 of the commonly-regulated genes, e.g. the tobacco orthologues
682 of *PUB26*, *RHC2A* and *DUF1,* encode proteins displaying ubiquitin ligase activity. Notably, *RHC2A* and
683 *DUF1* have been characterized as RING domain-containing E3 ubiquitin ligases (Kim et al. 2012).
684 Through their contribution in protein ubiquitination, ubiquitin ligases are main participants in protein
685 degradation pathways (Guerra & Callis, 2012). The observation that NO and ROS commonly regulates
686 genes predominantly related to protein ubiquitination is intriguing and, at this stage, we do not know
687 the physiological meaning of this finding. More generally, this data complete a recent study showing
688 that NO produced in response to cryptogein promotes the S-nitrosylation of the chaperone-like AAA+
689 ATPase CDC48 (Astier et al. 2012b). In animals and plants, CDC48 is involved in the targeting of
690 ubiquitinylated proteins for degradation by the proteasome (Meyer et al. 2012). Importantly, CDC48
691 has been shown to be similarly regulated by NO and ROS, both compounds promoting the S-
692 nitrosylation or oxidation on the same cysteine residue, respectively (Noguchi et al. 2005). Therefore,
693 taken together these data suggest that NO and ROS might be part of the regulation processes of the
694 ubiquitin system at the transcriptional and post-translational levels.

695 We previously provided first evidence that NO is one of the components involved in the
696 mechanisms underlying cryptogein-triggered cell death (Lamotte et al., 2004). In the present study,
697 we took advantage of the gp15 and CL5 cell suspensions to further investigate the role of both NO
698 and ROS in that process. Compared to wild type cells, the reduction of cell death observed in
699 cryptogein-treated gp15 cells indicates that ROS-derived from NtRBOHD activity might contribute to
700 cell death. Concerning NO, in wt cells its scavenging by cPTIO correlated with a 70% reduction in
701 cryptogein-triggered cell death. Scavenging of NO was also efficient in reducing cryptogein-induced
702 cell death in CL5 cells; however, to a lower extend (35% of reduction). This data was expected as
703 those cells generated 50% to 60% less NO as compared to control cells. Thus, the results obtained in
704 wt and CL5 cells favors a role for NO in cell death. In gp15 cells, the finding that cPTIO was inefficient
705 in suppressing the cell death mediated by the elicitor while these cells still generate NO suggests that
706 NO requires NtRBOHD activity for inducing cell death. If so, the lower production of ROS detected in
707 CL5 cells appears to be sufficient to forward NO into the cell death machinery. This hypothesis fits
708 well with previous studies highlighting that NO alone is not able to kill cells buts needs to cooperate
709 with ROS (Delledonne et al. 2001; de Pinto et al. 2002). More precisely, it has been proposed that NO
710 requires well balanced H_2O_2 levels to be channeled into the cell death pathway (Delledonne et al.
711 2001; Zago et al. 2006). Accordingly, compared to wt cells, the involvement of NO in mediating cell
712 death was minimized but still occurred in CL5 cells producing a low level of ROS.

713 Inevitably, our data raise the question of how NO and ROS derived from NADPH oxidase
714 promote cell death. In animals, $ONOO^-$ is known to act as a cytotoxic effector and mediator of
715 cellular injuries (Ferrer-Sueta et al. 2009). However, such role in cryptogein signaling is doubtful as
716 urate was previously reported to be ineffective in reducing the elicitor-mediated cell death (Lamotte
717 et al. 2004). More generally, it is commonly recognized that $ONOO^-$ is not an essential intermediate
718 in the processes underlying plant cell death (Delledonne et al. 2001; Zago et al. 2006). Similarly, the
719 list of genes regulated by both NO and ROS pointed out for a concerted action of both species in the
720 control of genes encoding proteins displaying ubiquitin ligase activities, but did not allow the
721 identification of genes previously reported as being involved in cell death such as Vacuolar
722 Processing Enzymes (Hara-Nishimura et al. 2005). Functional analysis of these genes should provide a
723 first view of the incidence of the synergism between NO and ROS derived from NtRBOHD. Finally,
724 another issue of this study is that NO and ROS are not the sole intermediates of cryptogein-induced
725 cell death. Indeed, the NO scavenger did not completely suppressed cell death in wt cells exposed to
726 cryptogein. Furthermore, scavenging of NO in elicitor-treated gp15 and CL5 cells did not severely
727 abolish the rate of cell death. Similarly, CL5 cells displayed a high rate of cells death while producing
728 a low amount of H_2O_2. Identification of the NO- and ROS-independent intermediates will require
729 further investigation.

To conclude, our study provide a detailed analysis of the interplays occurring between NO and ROS in a physiological context. Based on our data, we proposed the working model

ACKNOWLEDGEMENTS

This work was supported by La Région de Bourgogne (PARI AGRALE 8 project) and the Association Pour la Recherche sur les Nicotianées. AK was supported by a fellowship from La Région de Bourgogne (PARI AGRALE 8 project).

We would like to thank the following people for their precious help: Karim Bouhidel (UMR 1347 Agroécologie, Dijon, France), Lidwine Trouilh (plate-forme Biopuces, Génopole Toulouse Midi-Pyrénées, France), Delphine Pecqueur (plate-forme Protéomique CLIPP – CHU Dijon, France), Christian Brière (UMR 5546, Laboratoire de Recherche en Sciences Végétales, Toulouse, France) and Marc Lohse (Max-Planck-Institut für Molekulare Pflanzenphysiologie, Potsdam-Golm, Germany).

743 **REFERENCES**

744

745 Ahlfors R., Brosché M., Kollist H. & Kangasjärvi J. (2009) Nitric oxide modulates ozone-induced cell
746 death, hormone biosynthesis and gene expression in Arabidopsis thaliana. The Plant Journal 58, 1-12.

747

748 Alamillo J.M. & García-Olmedo F. (2001) Effects of urate, a natural inhibitor of peroxynitrite-
749 mediated toxicity, in the response of Arabidopsis thaliana to the bacterial pathogen Pseudomonas
750 syringae. The Plant Journal 25, 529-540.

751

752 Asai S. & Yoshioka H. (2009) Nitric oxide as a partner of reactive oxygen species participates in
753 disease resistance to nectrotophic pathogen *Botryis cinerea* in *Nicotiana benthamiana*. Molecular
754 Plant-Microbe Interaction 22, 619-629.

755

756 Astier J., Kulik A., Koen E., Besson-Bard A., Bourque S., Jeandroz S., Lamotte O. & Wendehenne D.
757 (2012a) Protein S-nitrosylation: what's going on in plants? Free Radical Biology and Medicine 53,
758 1101–1110.

759

760 Astier J., Besson-Bard A., Lamotte O., Bertoldo J., Bourque S., Terenzi H. & Wendehenne D. (2012b)
761 Nitric oxide inhibits the ATPase activity of the chaperone-like AAA+ATPase CDC48, a target for S-
762 nitrosylation in cryptogein signaling in tobacco cells. Biochemical Journal 447, 249–260.

763

764 Begara-Morales J.C., Chaki M., Sánchez-Calvo B., Mata-Pérez C., Leterrier M., Palma J.M., Barroso J.B.
765 & Corpas F.J. (2013) Protein tyrosine nitration in pea roots during development and senescence.
766 Journal of Experimental Botany 64, 1121-1134.

767

768 Bellin D., Asai S., Delledonne M. & Yoshioka H. (2013) Nitric oxide as a mediator for defense
769 responses. Molecular Plant-Microbe Interaction 26, 271-217.

770

771 Benjamini Y. & Hochberg Y. (1995) Controlling the false discovery rate: a practical and powerful
772 approach to multiple testing. Journal of the Royal Statistical Society, Series B57, 289-300.

773

774 Besson-Bard A., Pugin A. & Wendehenne D. (2008a) New Insights into nitric oxide signaling in plants.
775 Annual Review of Plant Biology 59, 21-39.

776

Besson-Bard A., Griveau S., Bedioui F. & Wendehenne D. (2008b) Real-time electrochemical detection of extracellular nitric oxide in tobacco cells exposed to cryptogein, an elicitor of defence responses. Journal of Experimental Botany 59, 3407–3414.

Besson-Bard A., Astier J., Rasul S., Wawer I., Dubreuil-Maurizi C., Jeandroz S. & Wendehenne D. (2009) Current view of nitric oxide-responsive genes in plants. Plant Science 177, 302–309.

Bonnet P., Bourdon E., Ponchet M., Blein J.P. & Ricci P. (1996) Acquired resistance triggered by elicitins in tobacco and other plants. European Journal of Plant Pathology 102, 181-192.

Bourque S., Dutartre A., Hammoudi V., Blanc S., Dahan J., Jeandroz J., Pichereaux C., Rossignol M. & Wendehenne D. (2011) Type-2 histone deacetylases as new regulators of elicitor-induced cell death in plants. New Phytologist 192, 127-139.

Bradford M. (1976) A rapid and sensitive method for the quantification of microgram quantities of proteins utilizing the principle of protein-dye binding. Analytical Biochemistry 72, 248-254.

Bright J., Desikan R., Hancock J.T., Weir I.S. & Neill S.J. (2006) ABA-induced NO generation and stomatal closure in Arabidopsis are dependent on H_2O_2 synthesis. The Plant Journal 45, 113-122.

Burza, A.M., Pekala, I., Sikora, J., Siedlecki, P., Małagocki, P., Bucholc, M., Koper, L., Zielenkiewicz, P., Dadlez, M. & Dobrowolska G. (2006) *Nicotiana tabacum* osmotic stress-activated kinase is regulated by phosphorylation on Ser-154 and Ser-158 in the kinase activation loop. Journal of Biological Chemistry 281, 34299-34311.

Cecconi D., Orzetti S., Vandelle E., Rinalducci S., Zolla L. & Delledonne M. (2009) Protein nitration during defense response in *Arabidopsis thaliana*. Electrophoresis 30, 2460-2468.

Chamnongpol S., Willekens H., Moeder W., Langebartels C., Sandermann H. Jr., Van Montagu M., Inzé D. & Van Camp W. (1998) Defense activation and enhanced pathogen tolerance induced by H_2O_2 in transgenic tobacco. Proceedings of the National Academy of Sciences of USA 95, 5818-5823.

Chandler M.T., Tandeau de Marsac N. & De Kouchkovsky Y. (1972) Photosynthetic growth of tobacco cells in liquid suspension. Canadian Journal of Botany 50, 2265-2270.

812 Corpas F.J., Palma J.M., del Río L.A. & Barroso J.B. (2009) Evidence supporting the existence of L-
813 arginine-dependent nitric oxide synthase activity in plants. New Phytologist 184, 9-14.
814
815 Courtois C., Besson A., Dahan J., Bourque S., Dobrowolska G., Pugin A. & Wendehenne D. (2008)
816 Nitric oxide signalling in plants: interplays with Ca^{2+} and protein kinases. Journal of Experimental
817 Botany 59, 155-163.
818
819 Dahan J., Pichereaux C., Rossignol M., Blanc S., Wendehenne D., Pugin A. & Bourque S. (2009)
820 Activation of a nuclear localized-SIPK in tobacco cells challenged by cryptogein, an elicitor of plant
821 defence reactions. Biochemical Journal 418, 191-200.
822
823 Delledonne M., Xia Y., Dixon R.A. & Lamb C. (1998) Nitric oxide functions as a signal in plant disease
824 resistance. Nature 394, 585-588.
825
826 Delledonne M., Zeier J., Marocco A. & Lamb C. (2001) Signal interactions between nitric oxide and
827 reactive oxygen intermediates in the plant hypersensitive disease resistance response. Proceedings
828 of the National Academy of Sciences of USA 98, 13454-13459.
829
830 Delledonne M., Polverari A. & Murgia I. (2003) The functions of nitric oxide-mediated signaling and
831 changes in gene expression during the hypersensitive response. Antioxidant and Redox Signaling 5,
832 33-41.
833
834 DeFalco T.A., Bender K.W. & Snedden W.A. (2010) Breaking the code: Ca^{2+} sensors in plant signalling.
835 Biochemical Journal 425, 27-40;
836
837 de Pinto M.C., Tommasi F. & De Gara L. (2002) Changes in the antioxidant systems as part of the
838 signaling pathway responsible for the programmed cell death activated by nitric oxide and reactive
839 oxygen species in tobacco Bright-Yellow 2 cells. Plant Physiology 130, 698-708.
840
841 Durner J., Wendehenne D. & Klessig D.F. (1998) Defense gene induction in tobacco by nitric oxide,
842 cyclic GMP, and cyclic ADP-ribose. Proceedings of the National Academy of Sciences of USA 95,
843 10328-10333.
844

845 Eulgem T., Weigman V.J., Chang H.-S., McDowell J.M., Holub E.B., Glazebrook J., Zhu T. & Dangl J.L.
846 (2004) Gene expression signatures from three genetically separable resistance gene signaling
847 pathways for downy mildew resistance. Plant Physiology 135, 1129-1144.
848
849 Ferrer-Sueta G. & Radi R. (2009) Chemical biology of peroxynitrite: kinetics, diffusion, and radicals.
850 ACS Chemical Biology 4, 161-177.
851
852 Foissner I., Wendehenne D., Langebartels C. & Durner J. (2000) *In vivo* imaging of an elicitor-induced
853 nitric oxide burst in tobacco. Plant Journal 23, 817-824.
854
855 Fuglsang A.T., Guo Y., Cuin T.A., Qiu Q., Song C., Kristiansen K.A., Bych K., Schulz A., Shabala S.,
856 Schumaker K.S., Palmgren M.G. & Zhu J.K. (2007) Arabidopsis protein kinase PKS5 inhibits the plasma
857 membrane H+ -ATPase by preventing interaction with 14-3-3 protein. Plant Cell 19, 1617-1634.
858
859 Gaupels F., Kuruthukulangarakoola G.T. & Durner J. (2011a) Upstream and downstream signals of
860 nitric oxide in pathogen defence. Current Opinion in Plant Biology 14, 707-714.
861
862 Gaupels F., Spiazzi-Vandelle E., Yang D. & Delledonne M. (2011b) Detection of peroxynitrite
863 accumulation in *Arabidopsis thaliana* during the hypersensitive defense response. Nitric Oxide 25,
864 222-228.
865
866 Gauthier A., Lamotte O., Reboutier D., Bouteau F., Pugin A. & Wendehenne D. (2007) Cryptogein-
867 induced anion effluxes: electrophysiological properties and analysis of the mechanisms through
868 which they contribute to the elicitor-triggered cell death. Plant Signaling and Behavior 2, 86-95.
869
870 Guerra D.D. & Callis J. (2012) Ubiquitin on the move: the ubiquitin modification system plays diverse
871 roles in the regulation of endoplasmic reticulum- and plasma membrane-localized proteins. Plant
872 Physiology 160, 56–64.
873
874 Gould K., Lamotte O., Klinguer A., Pugin A. & Wendehenne D. (2003) Nitric oxide production in
875 tobacco leaf cells: a generalized stress responses? Plant, Cell and Environment 26, 1851-1862.
876
877 Hara-Nishimura I., Hatsugai N., Nakaune S., Kuroyanagi M. & Nishimura M. (2005) Vacuolar
878 processing enzyme: an executor of plant cell death. Current Opinion in Plant Biology 8, 404-408.
879

880 Horchani F., Prévot M., Boscari A., Evangelisti E., Meilhoc E., Bruand C., Raymond P., Boncompagni E.,
881 Aschi-Smiti S., Puppo A. & Brouquisse R. (2011) Both plant and bacterial nitrate reductases
882 contribute to nitric oxide production in *Medicago truncatula* nitrogen-fixing nodules. Plant
883 Physiology 155, 1023-1036.
884
885 Hughes M.N. (2008) Chemistry of nitric oxide and related species. Methods in Enzymology 436, 3-19.
886
887 Jeandroz S., Lamotte O., Astier J., Rasul S., Trapet P., Besson-Bard A., Bourque S., Nicolas-Francès V.,
888 Ma W., Berkowitz G.A. & Wendehenne D. (2013) There's more to the picture than meets the eye:
889 Nitric oxide cross-talk with Ca^{2+} signaling. Plant Physiology, *in press*
890
891 Jourd'heuil D. (2002) Increased nitric oxide-dependent nitrosylation of 4,5-diaminofluorescein by
892 oxidants: implications for the measurement of intracellular nitric oxide. Free Radical Biology and
893 Medicine 33, 676-684.
894
895 Kim S.J., Ryu M.Y. & Kim W.T. (2012) Suppression of Arabidopsis RING-DUF1117 E3 ubiquitin ligases,
896 AtRDUF1 and AtRDUF2, reduces tolerance to ABA-mediated drought stress. Biochemical and
897 Biophysical Research Communications 420, 141–147.
898
899 Klessig D.F., Durner J., Noad R., Navarre D.A., Wendehenne D., Kumar D., Zhou J.M., Shah J., Zhang S.,
900 Kachroo P., Trifa Y., Pontier D., Lam E. & Silva H. (2000) Nitric oxide and salicylic acid signaling in plant
901 defense. Proceedings of the National Academy of Sciences of USA 97, 8849-8855.
902
903 Kulik A., Anielska-Mazur A., Bucholc M., Koen E., Szymańska K., Żmienko A., Krzywińska E., Wawer I.,
904 McLoughlin F., Ruszkowski D., Figlerowicz M., Testerink C., Skłodowska A., Wendehenne D. &
905 Dobrowolska G. (2012) SNF1-related protein kinases Type 2 are involved in plant responses to
906 cadmium stress. Plant Physiology 160, 868-883.
907
908 Laemmli U.K. (1970) Cleavage of structural proteins during the assembly of the head of
909 bacteriophage T4. Nature 227, 680-685.
910
911 Lamotte O., Gould K., Lecourieux D., Sequeira-Legrand A., Lebrun-Garcia A., Durner J., Pugin A. &
912 Wendehenne D. (2004) Analysis of nitric oxide signalling functions in tobacco cells challenged by the
913 elicitor cryptogein. Plant Physiology 135, 516-529.
914

915 Lecourieux D., Mazars C., Pauly N., Ranjeva R. & Pugin A. (2002) Analysis and effects of cytosolic free
916 calcium increases in response to elicitors in *Nicotiana plumbaginifolia* cells. Plant Cell 14, 2627-2641.
917
918 Lherminier J., Elmayan T., Fromentin J., Elaraqui K.T., Vesa S., Morel J., Verrier J.L., Cailleteau B., Blein
919 J.P. & Simon-Plas F. (2009) NADPH oxidase-mediated reactive oxygen species production: subcellular
920 localization and reassessment of its role in plant defense. Molecular Plant-Microbe Interaction 22,
921 868-881.
922
923 Libault M., Wan J., Czechowski T., Udvardi M., Stacey G. (2007) Identification of 118 Arabidopsis
924 transcription factor and 30 ubiquitin-ligase genes responding to chitin, a plant-defense elicitor.
925 Molecular Plant-Microbe Interactions 20, 900-911.
926
927 Lim M.H., Xu D. & Lippard S.J. (2006) Visualization of nitric oxide in living cells by a copper-based
928 fluorescent probe. Nature Chemical Biology 2, 375-380.
929
930 Lindermayr C. & Durner J. (2009) S-Nitrosylation in plants: pattern and function. Journal of
931 Proteomics 73, 1-9.
932
933 Lindermayr C., Sell S., Müller B., Leister D. & Durner J. (2010) Redox regulation of the NPR1-TGA1
934 system of *Arabidopsis thaliana* by nitric oxide. Plant Cell 22, 2894-2907.
935
936 Liu X.M., Nguyen X.C., Kim K.E., Han H.J., Yoo J., Lee K., Kim M.C., Yun D.J. & Chung W.S. (2013)
937 Phosphorylation of the zinc finger transcriptional regulator ZAT6 by MPK6 regulates Arabidopsis seed
938 germination under salt and osmotic stress. Biochemical and Biophysical Research Communications
939 430, 1054–1059
940
941 Mandal M.K., Chandra-Shekara A.C., Jeong R.D., Yu K., Zhu S., Chanda B., Navarre D., Kachroo A. &
942 Kachroo P. (2012) Oleic acid-dependent modulation of NITRIC OXIDE ASSOCIATED1 protein levels
943 regulates nitric oxide-mediated defense signaling in Arabidopsis. Plant Cell 24, 1654-1674.
944
945 Meyer H., Bug M. & Bremer S. (2012) Emerging functions of the VCP/p97 AAA-ATPase in the ubiquitin
946 system. Nature Cell Biology 14, 117-123.
947
948 Mittler R., Vanderauwera S., Suzuki N., Miller G., Tognetti V.B., Vandepoele K., Gollery M., Shulaev V.
949 & Van Breusegem F. (2011) ROS signaling: the new wave? Trends in Plant Science 16, 300-309.

950

951 Mur L.A., Laarhoven L.J., Harren F.J., Hall M.A. & Smith A.R. (2008) Nitric oxide interacts with
952 salicylate to regulate biphasic ethylene production during the hypersensitive response. Plant
953 Physiology 148, 1537-1546.

954

955 Noguchi M., Takata T., Kimura Y., Manno A., Murakami K., Koike M., Ohizumi H., Hori S. & Kakizuka A.
956 (2005) ATPase activity of p97/valosin-containing protein is regulated by oxidative modification of the
957 evolutionally conserved cysteine 522 residue in Walker A motif. Journal of Biological Chemistry 280,
958 41332-41341.

959

960 Ogawa T., Ueda Y., Yoshimura K. & Shigeoka S. (2005) Comprehensive analysis of cytosolic Nudix
961 hydrolases in *Arabidopsis thaliana*. Journal of Biological Chemistry 280, 25277-25283.

962

963 Ogawa T., Ishikawa K., Harada K., Fukusaki E., Yoshimura K. & Shigeoka S. (2009) Overexpression of
964 an ADP-ribose pyrophosphatase, AtNUDX2, confers enhanced tolerance to oxidative stress in
965 Arabidopsis plants. The Plant Journal 57, 289–301.

966

967 Palmieri M.C., Sell S., Huang X., Scherf M., Werner T., Durner J. & Lindermayr C. (2008) Nitric oxide-
968 responsive genes and promoters in *Arabidopsis thaliana*: a bioinformatics approach. Journal of
969 Experimental Botany 59, 177-186.

970

971 Parani M., Rudrabhatla S., Myers R., Weirich H., Smith B., Leaman D.W. & Goldman S.L. (2004)
972 Microarray analysis of nitric oxide responsive transcripts in Arabidopsis. Plant Biotechnology Journal
973 2, 359-366.

974

975 Perchepied L., Balagué C., Riou C., Claudel-Renard C., Rivière N., Grezes-Besset B. & Roby D. (2010)
976 Nitric oxide participates in the complex interplay of defense-related signaling pathways controlling
977 disease resistance to *Sclerotinia sclerotiorum* in *Arabidopsis thaliana*. Molecular Plant-Microbe
978 Interaction 23, 846-860.

979

980 Perraud A.L., Takanishi C.L., Shen B., Kang S., Smith M.K., Schmitz C., Knowles H.M., Ferraris D., Li W.,
981 Zhang J., Stoddard B.L. & Scharenberg A.M. (2005) Accumulation of free ADP-ribose from
982 mitochondria mediates oxidative stress-induced gating of TRPM2 cation channels. Journal of
983 Biological Chemistry 280, 6138-6148.

984

985 Piterková J., Petrivalský M., Luhová L., Mieslerová B., Sedlárová M. & Lebeda A. (2009) Local and
986 systemic production of nitric oxide in tomato responses to powdery mildew infection. Molecular
987 Plant Pathology 10, 501-513.
988
989 Pugin A., Frachisse J.M., Tavernier E., Bligny R., Gout E., Douce R. & Guern J. (1997) Early events
990 induced by the elicitor cryptogein in tobacco cells: involvement of a plasma membrane NADPH
991 oxidase and activation of glycolysis and the pentose phosphate pathway. Plant Cell 9, 2077-2091.
992
993 Rasul S., Dubreuil-Maurizi C., Lamotte O., Koen E., Poinssot B., Alcaraz G., Wendehenne D. &
994 Jeandroz S. (2012) Nitric oxide production mediates oligogalacturonides-triggered immunity and
995 resistance to *Botrytis cinerea* in *Arabidopsis thaliana*. Plant, Cell and Environment 35, 1483-1499.
996
997 Romero-Puertas M.C., Laxa M., Mattè A., Zaninotto F., Finkemeier I., Jones A.M., Perazzolli M.,
998 Vandelle E., Dietz K.J. & Delledonne M. (2007) S-nitrosylation of peroxiredoxin II E promotes
999 peroxynitrite-mediated tyrosine nitration. Plant Cell 19, 4120-4130.
1000
1001 Saito S., Yamamoto-Katou A., Yoshioka H., Doke N. & Kawakita K. (2006) Peroxynitrite generation and
1002 tyrosine nitration in defense responses in tobacco BY-2 cells. Plant and Cell Physiology 47, 689-697.
1003
1004 Schmidt G. W. & Delaney S. K. (2010) Stable internal reference genes for normalization of real-time
1005 RT-PCR in tobacco (*Nicotiana tabacum*) during development and abiotic stress. Molecular Genetics
1006 and Genomics 283, 233–241.
1007
1008 Serrano I., Romero-Puertas M.C., Rodríguez-Serrano M., Sandalio L.M. & Olmedilla A. (2012)
1009 Peroxynitrite mediates programmed cell death both in papillar cells and in self-incompatible pollen in
1010 the olive (*Olea europaea* L.). Journal of Experimental Botany 63, 1479-1493.
1011
1012 Setsukinai K., Urano Y., Kakinuma K., Majima H.J. & Nagano T. (2003) Development of novel
1013 fluorescence probes that can reliably detect reactive oxygen species and distinguish specific species.
1014 Journal of Biological Chemistry 278, 3170-3175.
1015
1016 Simon-Plas F., Rustérucci C., Milat M.L., Humbert C., Montillet J.L. & Blein J.P. (1997) Active oxygen
1017 species production in tobacco cells elicited by cryptogein. Plant, Cell and Environment 20, 1573-1579
1018

1019 Simon-Plas F., Elmayan T. & Blein J.P. (2002) The plasma membrane oxidase NtrbohD is responsible
1020 for AOS production in elicited tobacco cells. Plant Journal 31, 137-147.
1021
1022 Skelly M.J. & Loake G. (2013) Synthesis of redox-active molecules and their signalling functions during
1023 the expression of plant disease resistance. Antioxidant and Redox Signaling, *in press*.
1024
1025 Smyth G. K., (2004). Linear models and empirical Bayes methods for assessing differential expression
1026 in microarray experiments. Statistical Applications in Genetics and Molecular Biology, Vol 3, No. 1,
1027 Article 3
1028
1029 Song F. & Goodman R.M. (2001) Activity of nitric oxide is dependent on, but is partially required for
1030 function of, salicylic acid in the signaling pathway in tobacco systemic acquired resistance. Molecular
1031 Plant-Microbe Interaction 14, 1458-1462.
1032
1033 Srivastava N., Gonugunta V.K., Puli M.R. & Raghavendra A.S. (2009) Nitric oxide production occurs
1034 downstream of reactive oxygen species in guard cells during stomatal closure induced by chitosan in
1035 abaxial epidermis of *Pisum sativum*. Planta 229, 757-765.
1036
1037 Szczegielniak J., Borkiewicz L., Szurmak B., Lewandowska-Gnatowska E., Statkiewicz M., Klimecka M.,
1038 Cieśla J. &Muszyńka G. (2012) Maize calcium-dependent protein kinase (ZmCPK11): local and
1039 systemic response to wounding, regulation by touch and components of jasmonate signaling.
1040 Physiologia Plantarum 146, 1-14.
1041
1042 Tada Y., Spoel S.H., Pajerowska-Mukhtar K., Mou Z., Song J., Wang C., Zuo J. & Dong X. (2008) Plant
1043 immunity requires conformational changes of NPR1 via S-nitrosylation and thioredoxins. Science 321,
1044 952-956.
1045
1046 Takahashi H., Chen Z., Du H., Liu Y. & Klessig D.F. (1997) Development of necrosis and activation of
1047 disease resistance in transgenic tobacco plants with severely reduced catalase levels. Plant Journal
1048 11, 993-1005.
1049
1050 Vandelle E. & Delledonne M. (2011) Peroxynitrite formation and function in plants. Plant Science 181,
1051 534-539.
1052

1053 Vitecek J., Reinohl V. & Jones R.L. (2008) Measuring NO production by plant tissues and suspension
1054 cultured cells. Molecular Plant 1, 270-284.
1055
1056 Wawer I., Bucholc M., Astier J., Anielska-Mazur A., Dahan J., Kulik A., Wysłouch-Cieszynska A.,
1057 Zareba-Kozioł M., Krzywinska E., Dadlez M., Dobrowolska G. & Wendehenne D. (2010) Regulation of
1058 Nicotiana tabacum osmotic stress-activated protein kinase and its cellular partner GAPDH by nitric
1059 oxide in response to salinity. Biochemical Journal 429, 73-83.
1060
1061 Yamamoto-Katou A., Katou S., Yoshioka H., Doke N. & Kawakita K. (2006) Nitrate reductase is
1062 responsible for elicitin-induced nitric oxide production in *Nicotiana benthamiana*. Plant Cell and
1063 Physiology 47, 726-735.
1064
1065 Yoshioka H., Mase K., Yoshioka M., Kobayashi M. & Asai S. (2011) Regulatory mechanisms of nitric
1066 oxide and reactive oxygen species generation and their role in plant immunity. Nitric Oxide 25, 216-
1067 221.
1068
1069 Yun B.W., Feechan A., Yin M., Saidi N.B., Le Bihan T., Yu M., Moore J.W., Kang J.G., Kwon E., Spoel
1070 S.H., Pallas J.A. & Loake G.J. (2011) S-nitrosylation of NADPH oxidase regulates cell death in plant
1071 immunity. Nature 478:264-268.
1072
1073 Yun B.W., Spoel S.H. & Loake G.J. (2012) Synthesis of and signalling by small, redox active molecules
1074 in the plant immune response. Biochimical Biophysical Acta 1820, 770-776.
1075
1076 Zago E., Morsa S., Dat J.F., Alard P., Ferrarini A., Inzé D., Delledonne M. & Van Breusegem F. (2006)
1077 Nitric oxide- and hydrogen peroxide-responsive gene regulation during cell death induction in
1078 tobacco. Plant Physiology 141, 404-411.
1079
1080 Zhang S., Klessig D.F. (1997) Salicylic acid activates a 48-kD MAP kinase in tobacco. Plant Cell 9, 809–
1081 824.

1082 **TABLE 1. List of cryptogein-early induced genes regulated through a NO-depend process**

1083 Tobacco cell suspensions were pre-incubated with 500 µM cPTIO and then treated with 100 nM
1084 cryptogein for 30 min. Genes are sorted according to functional classes and fold changes. Tobacco
1085 genes sequences used for microarray analysis were annotated to *A. thaliana* on a base of the best
1086 matched SGN EST. FC: Fold change.

1087

Probe number	Accesion number	Gene name	Functional class	FC	pval. adj
A_95_P128872	At2g30360	CIPK11, PKS5, SNRK3.22, SIP4 (SOS3-interacting protein 4)	Signaling	4.10	0.0087
A_95_P201617	At2g15760	calmodulin-binding protein	Signaling	4.55	0.0078
A_95_P159542	At1g66920	serine/threonine protein kinase, putative	Signaling	4.69	0.0082
A_95_P297148	At4g33050	calmodulin-binding protein, EDA39	Signaling	4.82	0.0099
A_95_P254219	At5g47070	protein kinase, putative	Signaling	5.82	0.0079
A_95_P082790	At5g04340	C2H2, CZF2, ZAT6 (zinc finger of *A. thaliana* 6)	Signaling	4.42	0.0088
A_95_P138477	At1g49780	PUB26 (plant U-BOX 26)	Protein degradation	5.78	0.0088
A_95_P121687	At2g39720	RHC2A (RING-H2 finger C2A)	Protein degradation	4.25	0.0089
A_95_P139122	At3g46620	zinc finger (C3HC4-type RING finger), DUF1	Protein degradation	4.30	0.0079
A_95_P082445	At5g42650	CYP74A, DDE2, AOS (allene oxide synthase)	Hormones	5.68	0.0082
A_95_P162217	At2g41380	embryo-abundant protein-related	Development	6.57	0.0079
A_95_P060295	At5g47650	ATNUDX2, ATNUDT2 (*A. thaliana* nudix hydolase homolog 2)	Nucleotide metabolism	4.26	0.0094
A_95_P236459	At2g02520	unknown protein	Unclassified/unknown	4.05	0.0082
A_95_P136782	At5g11650	hydrolase, alpha/beta fold family protein	Unclassified/unknown	5.66	0.0079
A_95_P280708	At1g21380	VHS domain-containing protein / GAT domain-containing protein	Vesicle transport	7.70	0.0079

1088

1089

1090 **TABLE 2. List of cryptogein-early induced genes commonly regulated by both NO and ROS**

1091 Wild-type and gp15 cell suspensions were pre-incubated or not with 500 µM cPTIO and then treated
1092 with 100 nM cryptogein for 30 min. Levels of transcript accumulation was measured by qRT-PCR
1093 analysis. The data are presented as ratio of expression between cryptogein-treated and non-treated
1094 wt cells (wt), between cryptogein- and cryptogein + cPTIO-treated cells (cPTIO) and between
1095 cryptogein-treated and non-treated gp15 cells (gp15). The table presents results from three
1096 independent experiments. "- " means values with FC < 4. Statistical analysis (a,b) was done according
1097 to ANOVA followed by SNK test (P<0.05).

1098

Probe number / Gene name	**qRT-PCR (FC>4)**		
	wt	**cPTIO**	**gp15**
A_95_P128872 *CIPK11*	7.62 (a)	4.15 (b)	- (b)
A_95_P138477 *PUB26*	20.76 (a)	5.08 (b)	9.79 (b)
A_95_P121687 *RHC2A*	4.40 (a)	- (b)	-(b)
A_95_P139122 *DUF1*	5.54 (a)	- (b)	- (b)
A_95_P082790 *ZAT6*	6.50 (a)	-(b)	8.00 (a)

1099

1100

1101

1102 **FIGURE LEGENDS**

1103

1104 **Figure 1. Cryptogein-induced NO production is partly regulated through a NtRBOHD-dependent**
1105 **process**

1106 A. NO production in cryptogein-treated cells. Tobacco cell suspensions were first pre-incubated with
1107 500 µM cPTIO and then treated with 100 nM cryptogein. Graph present the time course of NO
1108 production measured using the intracellular NO-sensitive fluorophore DAF-2DA.

1109 B. Time course of H_2O_2 production in cryptogein-treated cells. Wild type and gp15 cells were treated
1110 with 100 nM cryptogein. The concentration of H_2O_2 of was measured by luminescence.

1111 C. Impact of NtRBOHD activity on cryptogein-mediated NO synthesis. Wild type and gp15 cells were
1112 pre-incubated or not with 5 µM DPI before cryptogein treatment (100 nM). Control cells were pre-
1113 treated with an equal volume of DMSO. The production of NO was measured after 40 min of
1114 cryptogein treatment using the intracellular NO-sensitive fluorophore DAF-2DA. The production of
1115 NO induced by cryptogein in wt cells in the absence of DMSO has been fixed at 100%.

1116 For each figures, each value represents the mean ± SE of nine measurements (three replicates per
1117 experiment performed three times). Statistical analysis was performed by ANOVA followed by SNK
1118 test ($P<0.05$).

1119

1120 **Figure 2. Incidence of NO on H_2O_2 level in cryptogein-treated cells**

1121 Tobacco cell suspensions were first pre-incubated with 500 µM cPTIO and then treated with 100 nM
1122 cryptogein. The production of H_2O_2 was measured by luminescence. The production of H_2O_2 induced
1123 by cryptogein in the absence of cPTIO has been fixed at 100%.

1124 Each value represents the mean ± SE of fifteen measurements (three replicates per experiment
1125 performed five times). Statistical analysis was performed by ANOVA followed by SNK test ($P<0.05$).

1126

1127 **Figure 3. Production of NO and H_2O_2 in CL5 cells elicited by cryptogein**

1128 A. Time course of H_2O_2 production in CL5 cells. Wild type and CL5 cells were treated with 100 nM
1129 cryptogein. The concentration of H_2O_2 was measured by luminescence.

1130 B. Intracellular NO production in CL5 measured with the DAF-2DA probe. Cells were treated with 100
1131 nM cryptogein for 40 min. The production of NO induced by cryptogein in wt cells has been fixed at
1132 100%.

1133 For each figure, each value represents the mean ± SE of nine measurements (three replicates per
1134 experiment performed three times). Statistical analysis was performed by ANOVA followed by SNK
1135 test ($P<0.05$).

1136

1137 **Figure 4. Cryptogein triggers a peroxynitrite production in tobacco cell suspensions**

1138 A. Analysis of APF responsiveness to $ONOO^-$. Wild type cells loaded with 5 µM APF were pre-
1139 incubated or not 5 min with 1 mM of the $ONOO^-$ scavenger urate (UA) and then with 2.5 mM SIN-1.
1140 Changes of APF fluorescence levels were monitored using a spectrofluorometer.

1141 B. Time course of $ONOO^-$ production in response to cryptogein-elicited cells. Wild type and gp15
1142 cells loaded with 5 µM APF were treated with 100 nM of cryptogein. Changes of APF level of
1143 fluorescence were monitored as indicated in Fig. 4A.

1144 C. Influence of urate on cryptogein-induced increase in APF fluorescence. Wild-type cells loaded with
1145 5 µM APF were pre-incubated or not 5 min with 1 mM of the $ONOO^-$ scavenger urate and then with
1146 100 nM of cryptogein. Changes of APF level of fluorescence were monitored as indicated in Fig. 4A.

1147 D. Cryptogein-induced $ONOO^-$ production in CL5 cells. Wild type and CL5 cells loaded with 5 µM APF
1148 were treated 40 min with 100 nM of cryptogein. Changes of APF level of fluorescence were
1149 monitored as indicated in Fig. 4A. The production of $ONOO^-$ induced by cryptogein in wt cells has
1150 been fixed at 100%.

1151 E. Cellular localization of $ONOO^-$. Wild type and gp15 cells were treated with cryptogein for 0, 20 and
1152 40 min and stained for 5 min with 15 µM APF. Peroxynitrite localization (green fluorescence) was
1153 observed with a confocal laser scanning microscope under magnification 40x. Chloroplast auto-
1154 fluorescence appears in red. The Figure is representative of pictures from six independent replicates
1155 with a minimum of 8 cells observed per conditions in each experiment. Scale bar mean 50 µM.
1156 Arrows indicate the position of the nucleus.

1157 For figures A-D, each value represents the mean ± SE of nine measurements (three replicates per
1158 experiment performed three times). For Fig. D, statistical analysis was performed by ANOVA followed
1159 by SNK test ($P<0.05$).

1160

1161 **Figure 5. ROS negatively regulate NtOSAK activity**

1162 Seven days-old wild type and gp15 cells were treated with 100 nM cryptogein for up to 9h. After
1163 proteins extraction, NtOSAK activity was monitored by immunocomplex-kinase activity assay using
1164 specific anti-C-terminal NtOSAK antibodies. Representative results from three independent
1165 experiments are presented.

1166

1167 **Figure 6. Peroxynitrite mitigated the expression of NO- and ROS-induced genes**

1168 Wild-type cell suspensions were pre-incubated or not with 1mM uric acid (UA) or 3.33 mM NaOH for
1169 10 min and then treated with 100 nM cryptogein for next 30 min. Levels of transcript accumulation
1170 was measured by qRT-PCR. The data are presented as ratio of expression between cryptogein-
1171 treated and not-treated cells; between cryptogein- and cryptogein + UA-treated cells; between

1172 cryptogein- and cryptogein + NaOH treated cells. Graphs present the results from three independent
1173 experiments. FC: fold change. Statistical analysis was done according to ANOVA followed by SNK test
1174 ($P<0.05$).
1175
1176 **Figure 7. Nitric oxide and ROS involvement in cryptogein-induced cell death**
1177 A. Involvement of NO and ROS in cryptogein-induced cell death in wt and gp15 cells. Cell suspensions
1178 were pre-treated for 10 min with 500 µM cPTIO before the addition of 100 nM cryptogein. The
1179 percentage of dead cells was estimated at the indicated time by staining with neutral red.
1180 B. Involvement of NO and ROS in cryptogein-induced cell death in CL5 cells. Cells were treated as
1181 detailed for Fig. 7A.
1182 For both figures, each value represents the mean ± SE of 6 measurements (2 replicates per
1183 experiment performed 3 times). Statistical analysis was done by ANOVA followed by SNK test
1184 ($P<0.05$).
1185
1186 **Figure 8**. Interplay between NO and ROS derived from NtRBOHD activity in cryptogein signaling
1187 The production of NO involves both NtRBOHD-dependent and -independent pathways. In the first
1188 one, both NO and ROS derived from NtRBOHD activity regulate a common set of genes including
1189 genes encoding proteins displaying putative ubiquitin ligase activities. Furthermore, NO involvement
1190 in cell death requires NtRBOHD activity. In turn, NO negatively regulates the level of H_2O_2, probably
1191 by forming peroxynitrite ($ONOO^-$) through its coupling with superoxide ($O_2^{\bullet-}$). In the NtRBOHD-
1192 independent pathway, NO regulates the expression of genes which products are related to signaling,
1193 hormone metabolism, vesicle transport and development. The regulation of NtOSAK activity in
1194 response to cryptogein specifically involves ROS but not NO. The role of NtOSAK is currently
1195 unknown.

1196 **SUPPORTING INFORMATION**

1197

1198 **Figure S1. NO production in cryptogein-treated cells tested by CuFL probe**

1199 NO production was measured after 40 min of cells treatment with 100 nM cryptogein. The
1200 production of NO induced by cryptogein has been fixed at 100%.

1201 A. Nitric oxide production in tobacco cells first pre-incubated with 500 µM cPTIO and then treated
1202 with elicitor.

1203 B. Incidence of NtRBOHD activity on cryptogein-mediated NO synthesis. The production of NO was
1204 measured in wt and gp15 cells after.

1205 C. Incidence of NtHDAC2a/b on cryptogein-mediated NO synthesis. The production of NO was
1206 measured in wt and CL5 cells after.

1207 Each value represents the mean ± SE of nine measurements (three replicates per experiment
1208 performed three times). Statistical analysis was performed by ANOVA followed by SNK test ($P<0.05$).

1209

1210 **Figure S2. DEA/NO induced DAF-2T fluorescence in the distinct cell lines**

1211 A. Time course of DAF-2T fluorescence in wt and gp15 cell suspensions exposed to the NO donor
1212 DEA/NO. Cells loaded with DAF-2DA were treated with 200 µM of DEA/NO or 200 µM DEA as control.

1213 B. Time course of DAF-2T fluorescence in wt and CL5 cell suspensions exposed to the NO donor
1214 DEA/NO. Cells loaded with DAF-2DA were treated with 200 µM of DEA/NO or 200 µM DEA as control.

1215 Graphs present one representative experiment of three. Bars mean ± SE (n = 3).

1216

1217 **Figure S3. Effect of DPI on cryptogein-induced H_2O_2 production**

1218 Cells were pre-incubated with 5 µM DPI (or equal volume of DMSO) for 5 min before cryptogein
1219 supply (100 nM). H_2O_2 levels were measured by luminescence. Each value represents the mean ± SE
1220 of 9 measurements (3 replicates per experiment performed 3 times).

1221

1222 **Figure S4. Cellular localization of NO**

1223 After filtration, seven days-old cells were equilibrated in H10 buffer for 1 h in 25°C in the dark and
1224 then stained for 1 h with 5 µM DAF-2DA. After three washes with fresh buffer, cells were equilibrated
1225 for next 30 min in new buffer and treated with 100 nM cryptogein for 0, 20 or 40 min. Cells were
1226 observed with a confocal laser scanning with settings and analysis of images as described for APF in
1227 Fig. 4E. The Figure is representative of pictures from four independent replicates with a minimum of
1228 8 cells observed per conditions in each experiment Scale bar mean 50 µM. Arrows indicate the
1229 position of the nucleus.

1230

1231

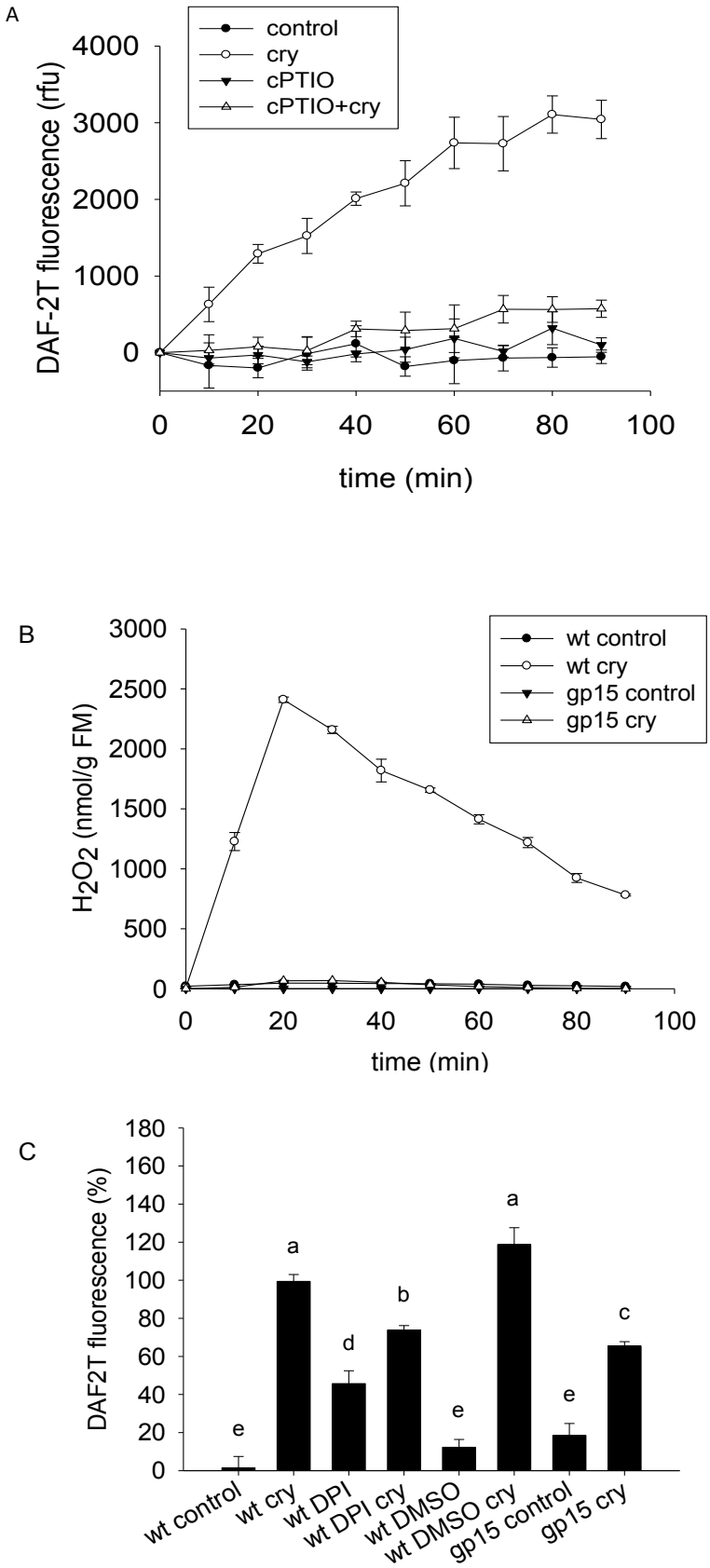

1232

1233

1234 **Figure 1**

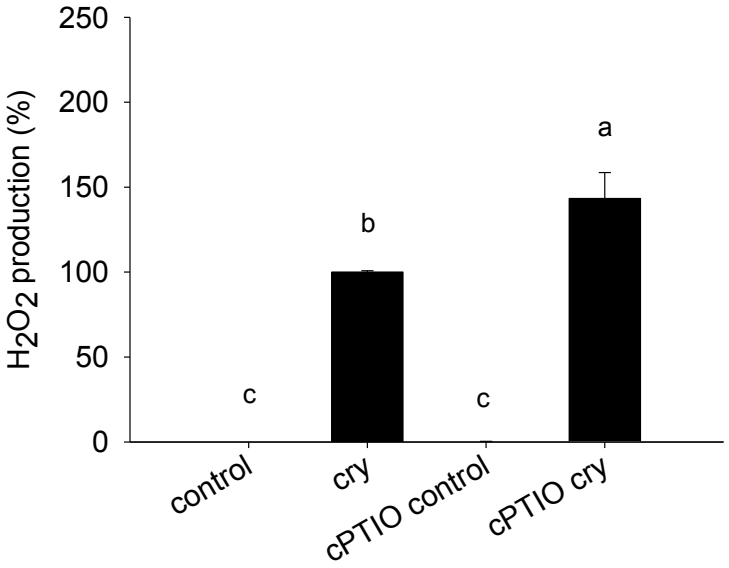

1235

1236 **Figure 2**

1237

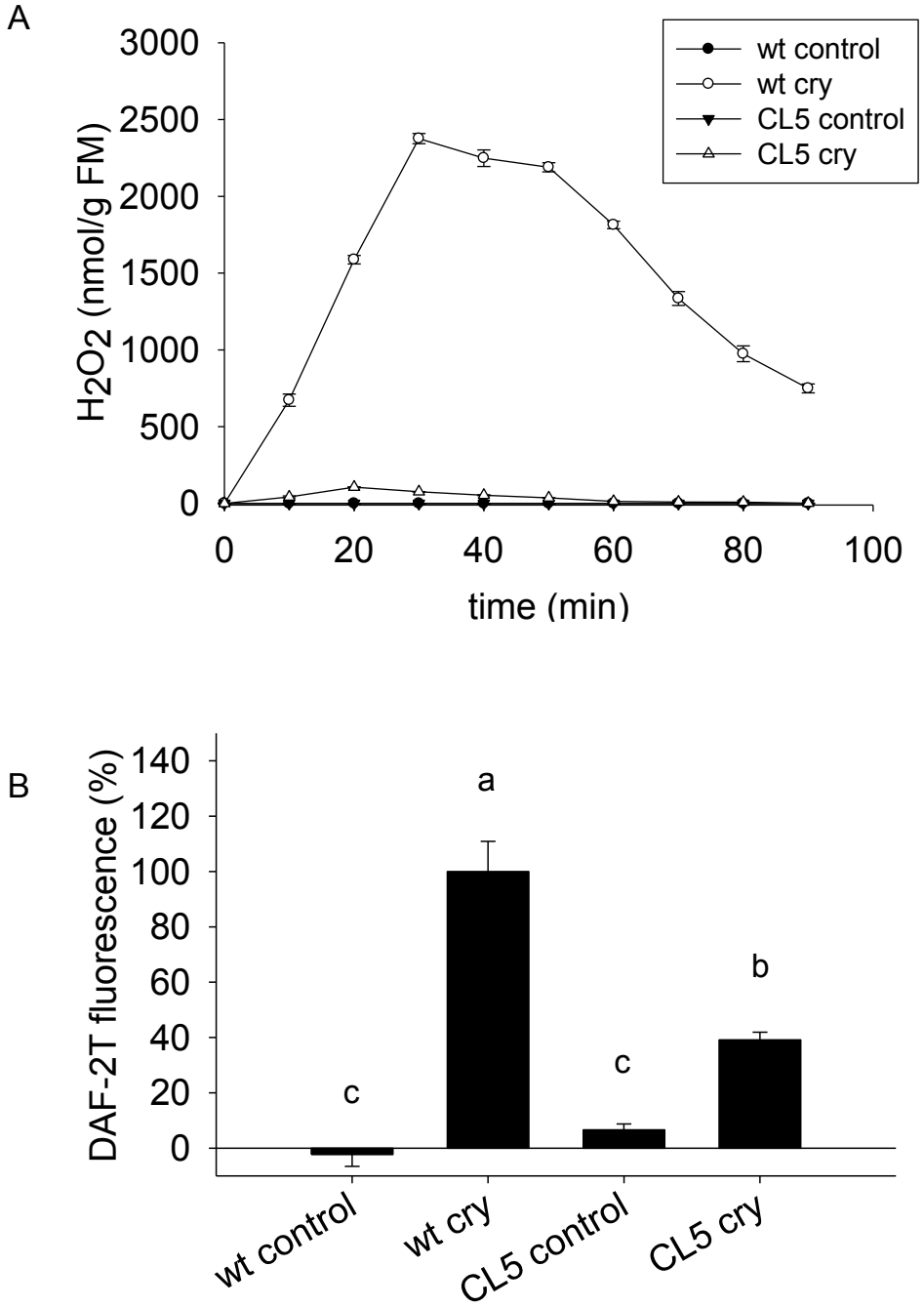

1238

1239 **Figure 3**

1240

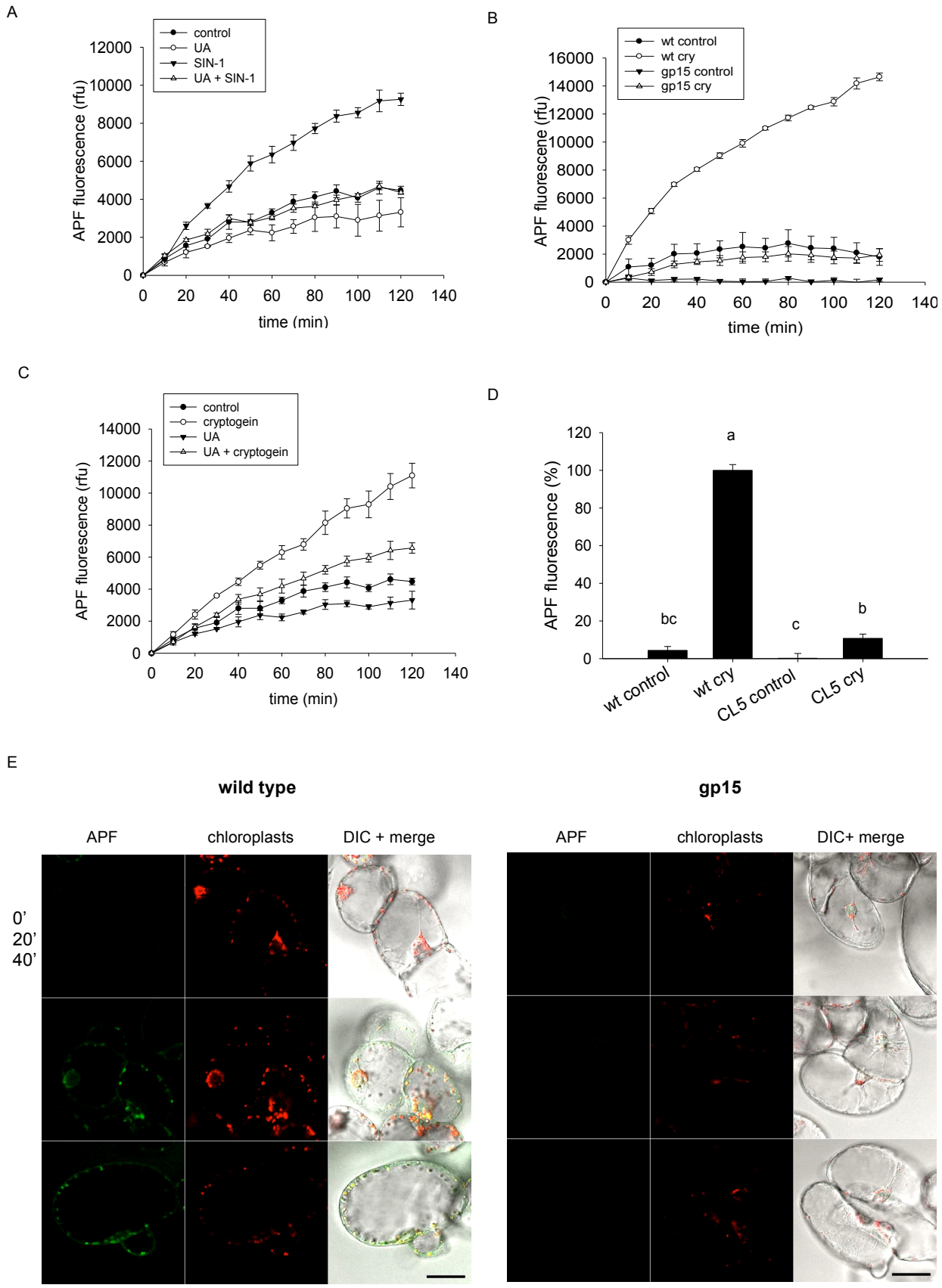
A
control
UA
SIN-1
UA + SIN-1
APF fluorescence (rfu)
time (min)
B
wt control
wt cry
gp15 control
gp15 cry
APF fluorescene (rfu)
time (min)
C
control
cryptogein
UA
UA + cryptogein
APF fluorescence (rfu)
time (min)
D
APF fluorescence (%)
a
bc
c
b
wt control
wt cry
CL5 control
CL5 cry
E
wild type
gp15
APF
chloroplasts
DIC + merge
DIC+ merge
0'
20'
40'

Figure 4

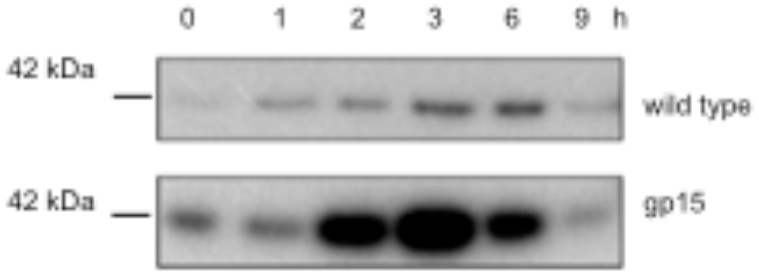

1245

1246

1247 **Figure 5**

1248

1249

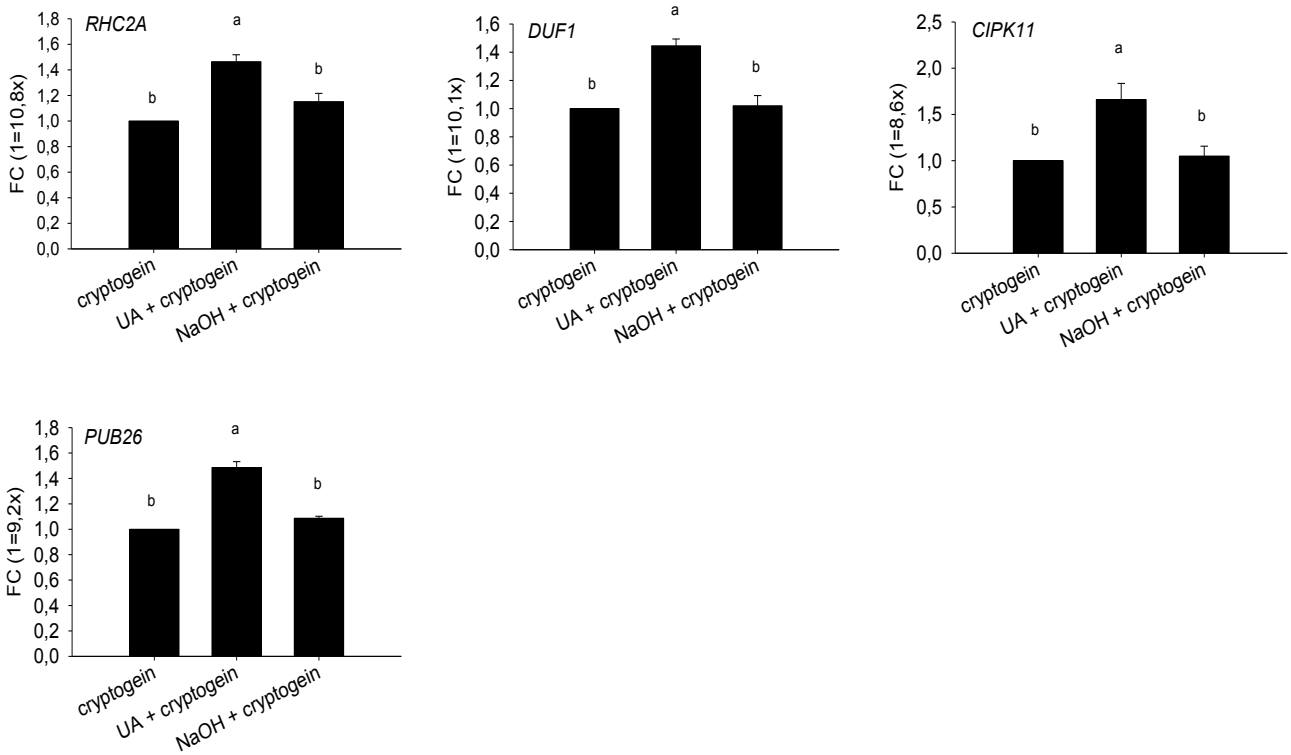

1250

1251 **Figure 6**

1252

1253

1254

1255

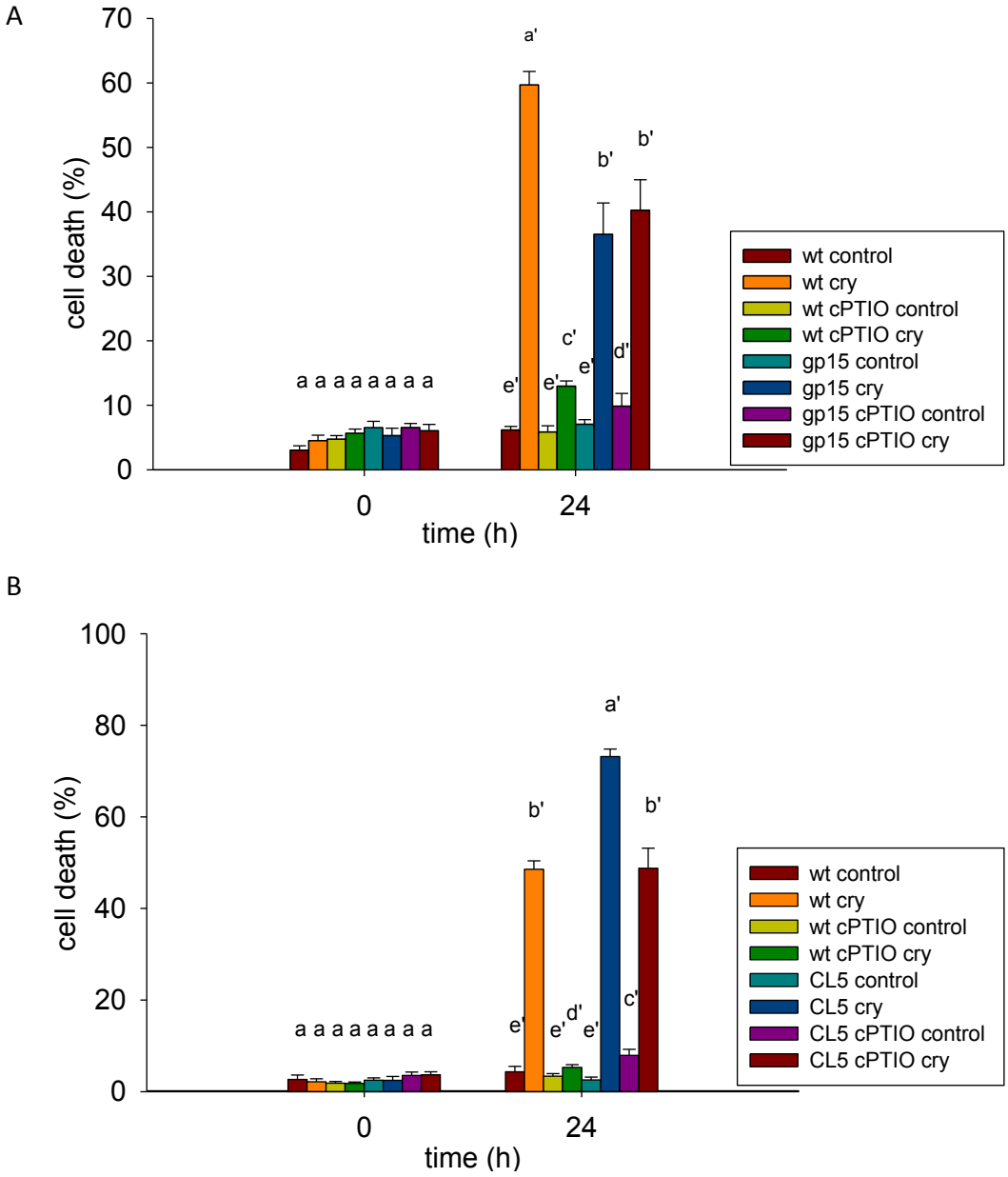

1277 **Figure 7**

1278

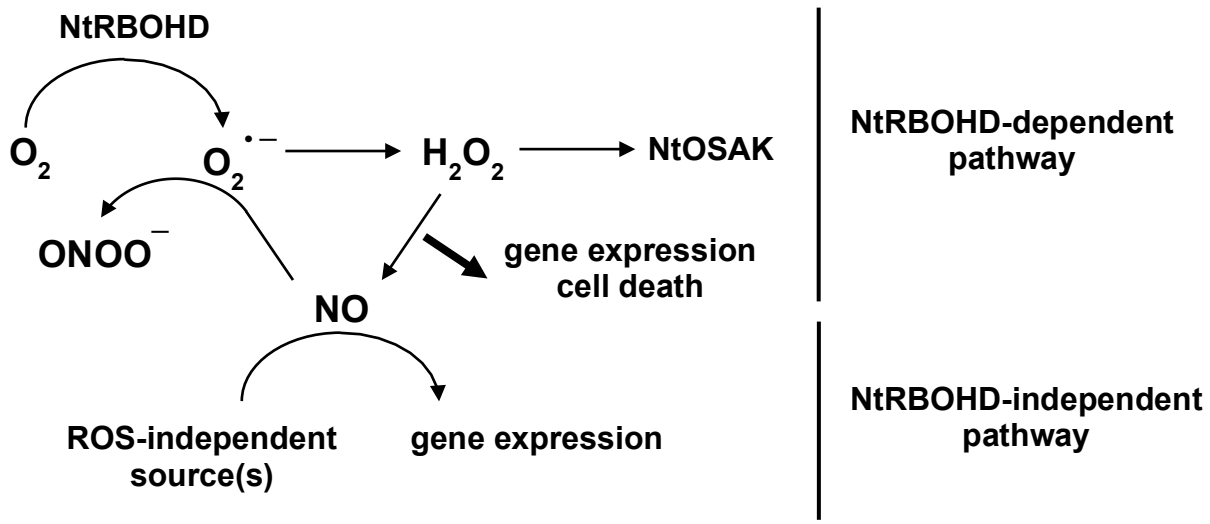

1279

1280

1281 **Figure 8**

1282

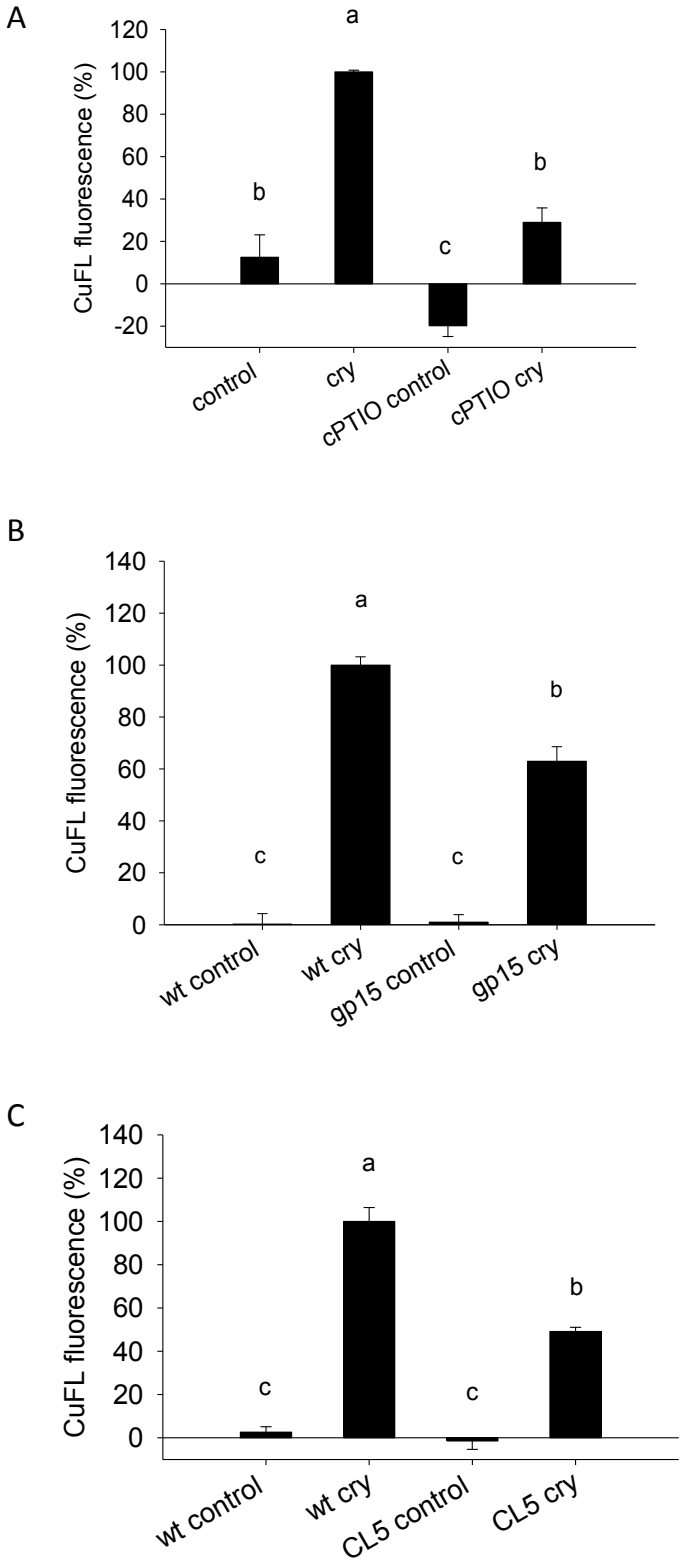
A
CuFL fluorescence (%)
120
100
80
60
40
20
0
-20
a
b
c
b
control
cry
cPTIO control
cPTIO cry
B
CuFL fluorescence (%)
140
120
100
80
60
40
20
0
a
b
c
c
wt control
wt cry
gp15 control
gp15 cry
C
CuFL fluorescence (%)
140
120
100
80
60
40
20
0
a
b
c
c
wt control
wt cry
CL5 control
CL5 cry

Figure S1

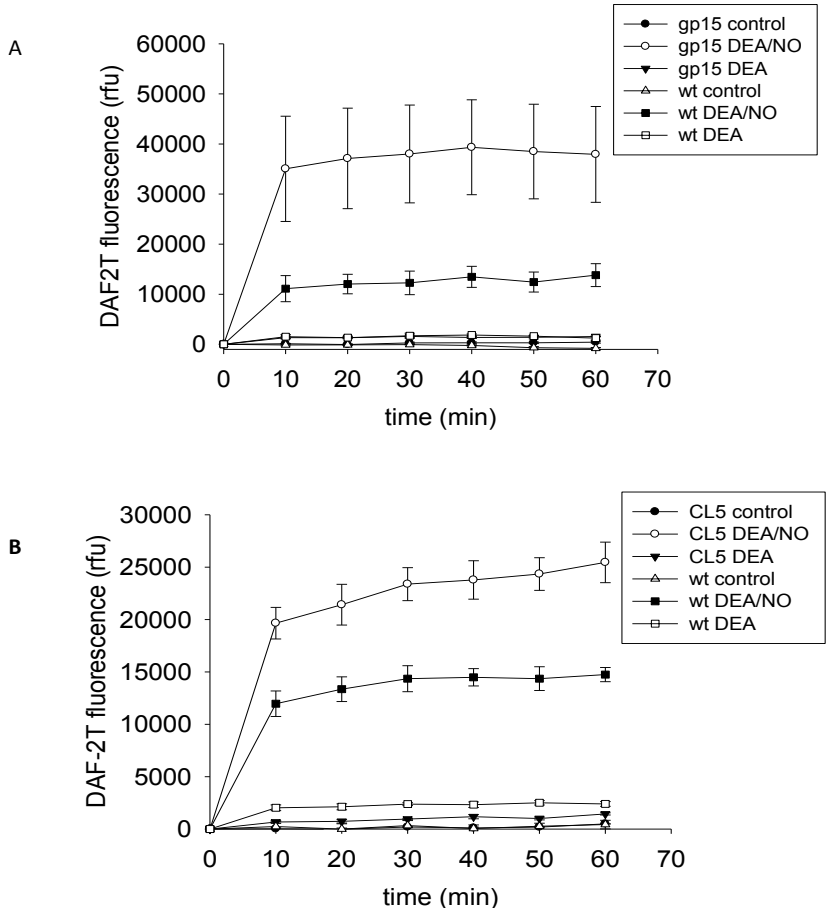

Figure S2

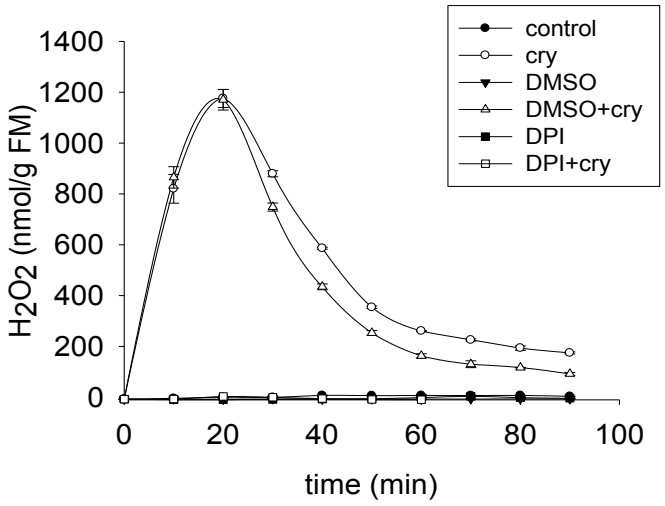

Figure S3

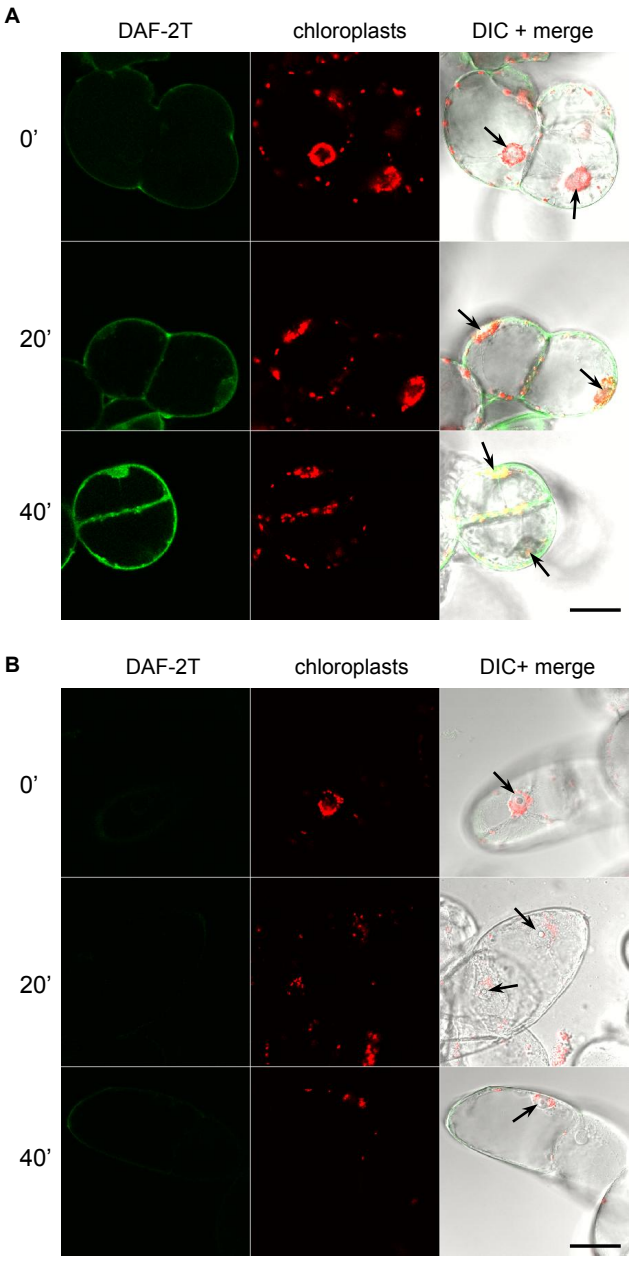

1337

1338

1339 **Figure S4**

1340

1341